Planet. Space Sci., Vol. 37, No. 4, pp. 427–458, 1989
Printed in Great Britain.

0032–0633/89 $3.00 + 0.00
Pergamon Press plc

AERONOMIC PROBLEMS OF MOLECULAR OXYGEN PHOTODISSOCIATION—V. PREDISSOCIATION IN THE SCHUMANN–RUNGE BANDS OF OXYGEN

MARCEL NICOLET,* S. CIESLIK† and ROBERT KENNES
Aeronomy Institute, 3 avenue Circulaire, B-1180 Brussels, Belgium

(*Received* 15 *December* 1988)

Abstract—New independent sets of laboratory absorption data for molecular oxygen provide sufficient spectral resolution in the Schumann–Runge region to yield line widths of the rotational lines. A definitive determination of the absorption cross-sections as a function of wavelength and temperature is possible. An analysis has been made of these new results to prepare a parameterization adapted to 500 cm^{-1} intervals for atmospheric conditions between 170 and 270 K in the mesosphere and stratosphere.

1. INTRODUCTION

Since 1969 (Ackerman *et al.*, 1969; Hudson and Carter, 1969; Hudson *et al.*, 1969), the number of publications on spectroscopic aspects (absorption, predissociation and photodissociation) of the ultraviolet spectrum (Herzberg systems and Schumann–Runge system) of molecular oxygen has been large. This is due to a geophysical fact, namely that the O_2 photodissociation by solar u.v. radiation between 175 and 242 nm is the source of ozone in the stratosphere and mesosphere, and that the O_2 absorption controls the atmospheric transmittance in this spectral region; i.e. it determines the differences in penetration of solar u.v. radiation at various wavelengths.

As pointed out by Nicolet and Mange (1954) precise knowledge of the absorption cross-sections in the bands of the O_2 Schumann–Runge system is needed for a detailed study of the penetration of solar radiation; this requires exact knowledge of the rotational line positions, with their line widths and oscillator strengths. The first detailed discussions of the implication of predissociation in the Schumann–Runge band system of O_2 were made by Ackerman and Biaumé (1970), Ackerman *et al.* (1970), Biaumé (1972a,b), Hudson and Mahle (1972), Allison *et al.* (1971) and Fang *et al.* (1974). Most recent published determinations of the predissociation line widths and the band oscillator strengths can be found in Frederick and Hudson (1979) and in various Australian papers (Lewis *et al.*, 1978, 1979, 1980, 1985a,b, 1986a,b,c; Gies *et al.*, 1981, 1982).

The incorporation of the cross-section data of the Schumann–Runge bands into atmospheric models has been made by different groups (Kockarts, 1971, 1976; Blake, 1979; Frederick and Hudson, 1980a,b; Nicolet and Cieslik, 1980; Nicolet and Peetermans, 1980; Nicolet, 1981, 1983, 1985; Allen and Frederick, 1982) in order to yield a simple parameterization of the interaction of solar radiation with O_2 and with other minor atmospheric gases in the mesosphere and stratosphere.

With regard to the Herzberg continuum, the first detailed laboratory measurements at relatively high pressures were made by Ditchburn and Young (1962), and then extrapolated to provide absorption cross-sections applicable to the stratosphere. The extension of this continuum below 200 nm into the spectral range of the bands of the Schumann–Runge systems was based on the theoretical determination of Jarmain and Nicholls (1967). Their theoretical curve was calibrated in terms of absolute values through use of the experimental data of Ditchburn and Young at wavelengths greater than 200 nm. The maximum absorption cross-section obtained near 195 nm is 1.3×10^{-23} cm^2. It is important to point out that, in their studies of atmospheric absorption in the Schumann–Runge bands all the authors (Ackerman *et al.* 1970; Hudson and Mahle, 1972; Fang *et al.*, 1974; Kockarts, 1976; Nicolet and Peetermans, 1980; Frederick and Hudson, 1980a,b) used the theoretical values of Jarmain and Nicholls, which are too high. If a mean value based on all experimental data (Ditchburn and Young, 1962; Ogawa, 1971; Hasson and Nicholls, 1971; Shardanand and Prasad Rao, 1977)

* Also, Communications and Space Sciences Laboratory, Penn State University, University Park, PA 16802, U.S.A.
† Now at Air Pollution Section, Chemistry Division, Ispra Establishment, Commission of the European Communities, Italy.

is used, there is a difference of a factor of 2 between the minimum and the maximum values. The lowest values obtained in the region 240–200 nm are those of Shardanand and Prasad Rao (1977). If they are used to calibrate the theoretical curve, the maximum absorption cross-section obtained at 195 nm is 10^{-23} cm^2. This difference has already been indicated by Blake (1979).

Balloon-borne spectrometer measurements of the solar irradiance in the stratosphere were analyzed by Frederick and Mentall (1982), Herman and Mentall (1982) and Anderson and Hall (1986). After correction for the atmospheric opacity due to ozone, they imply absorption cross-sections in the Herzberg continuum that are even smaller than those reported by Shardanand and Prasad Rao (1977).

Recent laboratory measurements made at Cambridge, Massachussetts (Cheung *et al.*, 1986), at Berkeley, California (Johnston *et al.*, 1984), and at Reims, France (Jenouvrier *et al.*, 1986) show that the absorption cross-section is less than 1×10^{-23} cm^2 at all wavelengths, and even of the order of 7.5×10^{-24} cm^2 at short wavelengths near 200 nm (Nicolet and Kennes, 1986). Comparison of the various experimental results reveals some disagreement which can be taken as indicative of the uncertainties in the available data. In any case, at wavelengths shorter than 200 nm, it is necessary to reduce the effect of the Herzberg continuum, particularly in the region of the 5–0 to 2–0 bands of the Schumann–Runge system. At still shorter wavelengths, i.e. for the 19–0 to 10–0 bands, it is also necessary to introduce absorption due to the Schumann–Runge continuum that occurs at wavelengths greater than 175 nm; it corresponds to an absorption by thermally excited molecules (300 K in the laboratory). After the first analysis made by Allison *et al.* (1971) and by Hudson and Mahle (1972) and developed by Blake (1979), the recent measurements made by Gies *et al.* (1982), Lewis *et al.* (1985a,b) must be used, because the continuum, a function of the temperature, has been divided into its constituent parts: absorption into the $B\,^3\Sigma_u^-$, $A\,^3\Sigma_u^+$ and $^3\Pi_g$ states.

With regard to laboratory work on the Schumann–Runge bands, the absorption cross-sections at 300 K that coincide with atomic silicon lines have been determined by Ackerman *et al.* (1970) and recently throughout the whole region 179.3–201.5 nm by Yoshino *et al.* (1983). An atlas of the Schumann–Runge absorption bands of O_2 in the wavelength region 175–205 nm has been published by Yoshino *et al.* (1984). Their rotational assignments are generally in agreement with those of Ackerman and Biaumé (1970) and Brix and Herzberg (1954).

Finally, two recent publications (Nicolet *et al.*, 1987, 1988) describe the results obtained by a theoretical determination of the rotational structure and absolute absorption cross-sections of the O_2 Schumann–Runge bands between 300 and 79 K. This determination was based on the most recent experimental results. In the present paper the various spectroscopic parameters adopted to obtain the numerical values are provided for all possible calculations.

2. EXPERIMENTAL DATA ON ABSORPTION CROSS-SECTIONS

The absorption spectrum of the Schumann–Runge bands is characterized by various spectral intervals that correspond to the 20 bands 0–0 to 19–0. The adopted spectral limits cover the region from 49,000 to 57,035 cm^{-1}, i.e. from 204 to 175 nm (Table 1).

The experimental absolute cross-section data have been determined at 300 and at 79 K with a bandwidth of 0.4 cm^{-1} in the wavelength region 179–201 nm corresponding to the $v' = 1$–12 bands by Yoshino *et al.* (1983, 1987). These detailed measurements have been adopted for our aeronomic determination.

The positions of the lines within the Schumann–Runge bands have been calculated by using experimentally determined molecular constants, classical formulae yielding the energies of the quantum levels and sublevels and the selection rules for $a\,^3\Sigma_u^- - {}^3\Sigma_g^-$ transition in a homonuclear molecule. The energies of the spin–split rotational levels of $^3\Sigma$ can be expressed by the formulae of Miller and Townes (1953)

$$E_1(v,J) = T_v + B_v X - D_v X^2 - (\lambda_v - B_v + \tfrac{1}{2}\gamma_v) - [(\lambda_v - B_v + \tfrac{1}{2}\gamma_v)^2 + 4X(B_v + \tfrac{1}{2}\gamma_v)^2]^{1/2}$$

$$E_2(v,J) = T_v + B_v X - D_v X^2$$

$$E_3(v,J) = T_v + B_v X - D_v X^2 - (\lambda_v - B_v + \tfrac{1}{2}\gamma_v) + [(\lambda_v - B_v + \tfrac{1}{2}\gamma_v)^2 + 4X(B_v - \tfrac{1}{2}\gamma_v)^2]^{1/2}$$

for each component of the triplet. The meaning of the symbols are as follows:

$X = J(J+1)$, where J is the total angular momentum quantum number;
T_v is the vibrational term value;
B_v is the rotational constant;
D_v is the centrifugal distorsion constant;
λ_v is the interaction constant between the spins of the unpaired electrons;
γ_v is the interaction constant between the resultant electron spin and the magnetic moment produced by the rotation of the molecule.

TABLE 1. ADOPTED SPECTROSCOPIC CONSTANTS FOR THE UPPER STATE OF THE SCHUMANN–RUNGE BANDS OF O_2 TO COMPUTE LINE POSITIONS

Band	v_0 (cm^{-1})	B_v	D_v	λ_v	γ_v
0–0	49357.96	0.8132	4.50×10^{-6}	1.69	-2.80×10^{-2}
1–0	50045.53	0.7993	4.20×10^{-6}	1.70	-2.60×10^{-2}
2–0	50710.68	0.7860	5.80×10^{-6}	1.69	-2.90×10^{-2}
3–0	51351.94	0.7705	5.20×10^{-6}	1.70	-2.60×10^{-2}
4–0	51969.36	0.7550	5.97×10^{-6}	1.81	-3.00×10^{-2}
5–0	52560.94	0.7377	5.80×10^{-6}	1.75	-2.20×10^{-2}
6–0	53122.65	0.7187	5.00×10^{-6}	1.79	-2.10×10^{-2}
7–0	53655.95	0.7010	8.60×10^{-6}	1.82	-2.10×10^{-2}
8–0	54156.22	0.6770	6.70×10^{-6}	1.91	-2.30×10^{-2}
9–0	54622.50	0.6514	6.30×10^{-6}	2.04	-2.10×10^{-2}
10–0	55051.16	0.6263	9.90×10^{-6}	2.10	-4.10×10^{-2}
11–0	55439.23	0.5956	9.40×10^{-6}	2.17	-3.80×10^{-2}
12–0	55784.58	0.5626	1.37×10^{-5}	2.37	-5.40×10^{-2}
13–0	56085.44	0.5242	1.63×10^{-5}	2.51	-8.40×10^{-2}
14–0	56340.42	0.4832	2.09×10^{-5}	2.81	-1.16×10^{-1}
15–0	56550.62	0.4391	2.54×10^{-5}	3.30	-1.64×10^{-1}
16–0	56719.62	0.3934	3.08×10^{-5}	4.11	-2.41×10^{-1}
17–0	56852.45	0.3457	3.34×10^{-5}	5.18	-3.48×10^{-1}
18–0	56951.60	0.2872	5.50×10^{-5}	6.51	-4.94×10^{-1}
19–0	57025.80	0.2649	6.00×10^{-5}	7.63	-6.04×10^{-1}

v_0 = band origin = $T+\frac{2}{3}\lambda-\gamma$ as given by Cheung *et al.* (1986).
B_v and D_v = rotational constants for vibrational levels.
λ_v and γ_v splitting constants for vibrational levels.
For 18–0 and 19–0, see Fang *et al.* (1974).

The numerical values listed previously (Nicolet *et al.*, 1988) for these molecular constants are reproduced in Table 1 for the $v''=0$ of the $X^3\Sigma_g^-$ ground state and for the $v'=0$–19 levels of the $B\ ^3\Sigma_u^-$ excited state.

For calculation of the level energies, we have used the Hund's case (b) representation, in which these energies are expressed in terms of the quantum number N instead of J, because the electronic states involved in the transition through Hund's intermediate coupling case are closer to the (b) than to the (a) case. The quantum numbers J and N are related by $J=N+S$, yielding $N=J-1$, J and $J+1$ for the spin components to triplet states.

Since O_2 is a homonuclear molecule (we restricted this study to the normal ^{16}O–^{16}O form), only symmetrical rotational levels exist, characterized by odd values of $N(=1,3,5,\ldots)$ for the lower state, and by even values of $N(=2,4,6,\ldots)$ for the upper state, as shown in the rotational analysis of the Schumann–Runge system performed by Brix and Herzberg (1954). Tatum and Watson (1971) showed that 14 branches may theoretically exist in a $^3\Sigma^\pm$–$^3\Sigma^\pm$ transition: six are the so-called principal branches, with $\Delta J=\Delta N(P_{11}, P_{22}$, and $P_{23}; R_{11}, R_{22}$ and $R_{33})$; the other eight are the satellite branches with $\Delta J\neq\Delta N(^RP_{13}, {}^NP_{13}, {}^PQ_{12}, {}^PQ_{23}, {}^RQ_{32}, {}^RQ_{21}, {}^PR_{13}$ and $^TR_{31})$.

3. LINE INTENSITIES

For simplicity, we use the term "line intensity" in designating the quantity which should correctly be termed the "line integrated absorption cross-section", and which is defined by

$$S_L=\int_0^\infty \sigma_L(v)\,dv$$

where v is the frequency (cm^{-1}) and σ_L is the contribution of the L-labelled line to the total absorption cross-section.

A dimensionless parameter, the line oscillator strength f, is introduced, and is related to S_L by

$$S_L=\frac{\pi e^2}{mc^2}\cdot f_L\cdot F(v'',N'')$$

where e and m are the electric charge and the mass, respectively, of the motionless electron, c is the velocity of light, and $F(v'',N'')$ is the relative population of the lower state of the transition. In the case of a rotational line within a triplet–triplet band, the line oscillator strength is given by

$$f_L=f_{N'N''}=f_{v'v''}\cdot\frac{S_{N'N''}}{3(2N''+1)}$$

where $f_{v'v''}$ is the band oscillator strength and $S_{N'N''}$ is the rotational line strength factor, also known as

the Hönl–London factor. The denominator is a normalization factor arising from degeneracy of the states.

4. BAND OSCILLATOR STRENGTH

The band oscillator strength $f_{v'v''}$ can be determined experimentally, and considerable work has been devoted to the determination of those of the Schumann–Runge bands. These bands, analyzed many times, are best resolved by the recent wavenumber measurements of Yoshino *et al.* (1984). Their comprehensive analysis based on Yoshino *et al.* (1983) yields a determination of mean band oscillator strengths from 0–0 to 12–0. Another approach by Lewis *et al.* (1986a,b,c) that reveals a variation of the oscillator strength with the rotational lines, is, however, in agreement with the high resolution measurements, when a mean value is adopted for the oscillator strength. Since it is practically impossible to adopt an *exact* oscillator strength for each line, equivalent values for each vibration level must be determined. The mean band oscillator strengths adopted here are based on the results of the Cambridge and Canberra groups and are used to generate a consistent set of data given in Table 2. These mean band oscillator strengths can therefore be used for the determination of the line widths of the rotational lines in the various Schumann–Runge bands. It seems that the oscillator strengths are generally accurate to about 5%, at least for bands with v' less than 15; attempts which have been made to study the possible errors have not produced more accurate oscillator strengths within the appropriate uncertainty.

TABLE 2. ADOPTED MEAN ABSORPTION OSCILLATOR STRENGTHS $f_{v''v'}$ FOR THE SCHUMANN–RUNGE BANDS OF O_2 DEDUCED FROM ABSORPTION SPECTRA

v'	$f_{0v'}$	$f_{1v'}$
0	2.8×10^{-10}	7.6×10^{-9}
1	3.0×10^{-9}	8.2×10^{-8}
2	1.9×10^{-8}	4.6×10^{-7}
3	8.2×10^{-8}	1.8×10^{-6}
4	2.7×10^{-7}	5.0×10^{-6}
5	7.4×10^{-7}	1.3×10^{-5}
6	1.6×10^{-6}	2.7×10^{-5}
7	3.4×10^{-6}	5.0×10^{-5}
8	6.2×10^{-6}	8.6×10^{-5}
9	1.0×10^{-5}	1.2×10^{-4}
10	1.5×10^{-5}	1.7×10^{-4}
11	1.9×10^{-5}	2.1×10^{-4}
12	2.4×10^{-5}	2.6×10^{-4}
13	2.7×10^{-5}	2.6×10^{-4}
14	2.8×10^{-5}	2.9×10^{-4}
15	2.7×10^{-5}	2.7×10^{-4}
16	2.6×10^{-5}	2.0×10^{-4}
17	2.2×10^{-5}	1.6×10^{-4}
18	1.7×10^{-5}	1.3×10^{-4}
19	1.3×10^{-5}	1.6×10^{-4}

5. ROTATIONAL DISTRIBUTION

The $S_{N'N''}$-factors, which govern the rotational intensity distribution in a band, have different algebraic forms for the branches of the band; they depend also on the type of transition. For the $^3\Sigma^{\pm}$–$^3\Sigma^{\pm}$ transitions, the explicit formulae for the $S_{N'N''}$ derived by Tatum and Watson (1971) are used here.

The relative populations of the lower states are given by the Boltzmann distribution:

$$F(v'',N'') = 3(2N''+1)\cdot\frac{\exp\left\{-\dfrac{hcE(v'',N'')}{kT}\right\}}{\sum\limits_{v''}\sum\limits_{N''}\exp\left\{-\dfrac{hcE(v'',N'')}{kT}\right\}}$$

where h and k are the Planck and Boltzmann constants, respectively, and T is the temperature. The sum (sum of state or partition function) which appears in the denominator can be limited to $v''=0$ and 1 for the vibration and to $N''<30$ for the rotation, since the temperature does not exceed 300 K in our calculations.

6. ABSORPTION CROSS-SECTION

The absorption cross-section at a given wavenumber is theoretically given by

$$\sigma(\nu) = \sigma_c(\nu)+\Sigma\sigma_L(\nu)$$

where $\sigma_c(\nu)$ is the contribution of the underlying continuum and the sum extends over all the lines of the spectrum. Obviously, only part of the lines are used, excluding those for which the line center ν_L is too far from the wavenumber ν. In our calculation, a given line is used in the preceding formula if it satisfies the condition

$$|\nu-\nu_L| < \Delta$$

where Δ is a spectral interval to be defined. Particular attention was paid to the choice of Δ since the lines may be quite broad in certain parts of the Schumann–Runge band spectrum; in the final computation we used values of Δ of 500 cm^{-1}.

In fact, to determine the exact contribution of the lines to the cross-section, a number of runs were made with increasing values of Δ (ranging from 100 to 500 cm^{-1}). When the result does not depend on Δ, this

means that the exact contribution of the lines is known; 500 cm^{-1} was adopted for the spectral interval Δ at each 0.1 cm^{-1}.

The contributions $\sigma_L(\nu)$ of the individual lines have been calculated using the Voigt profile approximated by a formula established by Whiting (1968):

$$\frac{\sigma_L(\nu)}{\sigma_L(\nu_L)} = \left(1-\frac{\Delta\nu_L}{\Delta\nu_v}\right)\exp\left\{-2.772\left(\frac{\nu-\nu_L}{\Delta\nu_v}\right)\right\} + \frac{(\Delta\nu_L/\Delta\nu_v)}{1+4\left(\frac{\nu-\nu_L}{\Delta\nu_v}\right)^{2.25}} + 0.016\left(1-\frac{\Delta\nu_L}{\Delta\nu_v}\right)\left(\frac{\Delta\nu_L}{\Delta\nu_v}\right) \cdot \left[\exp\left\{-0.4\left(\frac{\nu-\nu_L}{\Delta\nu_v}\right)^{2.25}\right\} - \frac{10}{10+\frac{\nu-\nu_L}{\Delta\nu_v}}\right]$$

where $\sigma_L(\nu_L)$ is the absorption cross-section at the centre of the line and is given by

$$\sigma_L(\nu_L) = \frac{S_L}{\Delta\nu_v\left[1.065+0.447\left(\frac{\Delta\nu_L}{\Delta\nu_v}\right)+0.058\left(\frac{\Delta\nu_L}{\Delta\nu_v}\right)\right]}$$

$\Delta\nu_v$ is the Voigt line width, given by

$$\Delta\nu_v = \frac{\Delta\nu_L}{2} + \left[\frac{\Delta\nu_L^2}{4} + \Delta\nu_D^2\right]^{1/2}$$

where $\Delta\nu_L$ is the Lorentz line width and $\Delta\nu_D$ is the Doppler line width. The Doppler line width can be calculated by

$$\Delta\nu_D = 7.1623\cdot 10^{-7}\nu_L\left(\frac{T}{M}\right)^{1/2}$$

where $M = 32$ is the molecular weight.

7. ROTATIONAL PREDISSOCIATION LINEWIDTHS

The mean predissociation line widths (Table 3) were determined after a detailed comparison between calculated absorption cross-sections and the experimental results published by Yoshino *et al.* (1983) in the spectral region corresponding to the $v' = 1$–12 bands. Furthermore, the absorption cross-sections throughout this region also depend on the underlying continuum that corresponds near 50,000 cm to the O_2 Herzberg continuum. At wavenumbers greater than 55,000 cm^{-1}, the O_2 Schumann–Runge continuum (Lewis *et al.*, 1985a,b) plays a role that is dependent on temperature. These two underlying continua are described in an atlas in Nicolet *et al.* (1987). In this publication, tables and figures of calculated absorption cross-sections are given for molecular oxygen as a function of wavenumber over the spectral interval 49,000–57,000 cm^{-1} for temperatures between 190 and 300 K.

TABLE 3. ADOPTED MEAN ROTATIONAL LINE WIDTHS

v'	cm^{-1}	v'	cm^{-1}
0	0.1	10	1.0
1	0.9	11	1.4
2	0.6	12	0.8
3	1.8	13	0.5
4	3.6	14	0.5
5	2.0	15	0.5
6	1.8	16	0.5
7	1.9	17	0.5
8	2.1	18	0.3
9	1.2	19	0.3

8. THE 500 CM^{-1} SPECTRAL INTERVALS

Various calculations were made for the different spectral intervals, but as usual the 500 cm^{-1} wave number grid was adopted finally. Such an interval corresponds to a constant energy range and is the most appropriate; it is very practical for atmospheric modeling because the solar irradiance is not known with high accuracy and its spectral resolution is generally inadequate for a study with detailed structure. Thus, it seems useful to describe the principal features in each of 17 intervals between 49,000 and 57,000 cm^{-1}. Such description provides a first indication of the strong variation of the absorption from 200 to 175 nm, and the relative effects of the underlying continuum.

8.1. *The spectral interval* 49,000–49,500 cm^{-1}

This interval corresponds to the spectral region of the 0–0 and 2–1 bands with minimum absorption cross-sections less than 10^{-26} cm^2, and even less than 10^{-27} cm^2 at low temperature. Thus, the averaged cross-section depends strongly on the underlying continuum. The Herzberg continuum absorption cross-section must be known with great accuracy and can be determined experimentally at low temperature in the spectral region of $v' = 1$ bands. It is of the order of 7×10^{-24} cm^2.

8.2. *The spectral interval* 49,500–50,000 cm^{-1}

The 1–0 and 3–1 bands are the principal bands within this spectral interval, with minimum cross-sections at low temperature less than 10^{-26} cm^2 between 49,500 and 49,750 cm^{-1}, and less than 10^{-25} cm^2 between 49,750 and 50,000 cm^{-1}. The Herzberg con-

tinuum makes the principal contribution to the determination of the averaged cross-section, particularly in the 49,500–49,750 spectral interval, because its own cross-section is not less than 7×10^{-24} cm^2.

A first comparison between the *experimental* and *theoretical* absorption cross-sections at 300 K can be made in the 49,750–50,000 cm^{-1} region, particularly with the peaks of the rotational lines of the 1–0 band. It is clear, however, that experimental noise persists at cross-sections of the order of 10^{-23} cm^2 so that a comparison with the Herzberg continuum cannot be made between the rotational lines.

8.3. *The spectral interval* 50,000–50,500 *cm*$^{-1}$

This region is characterized by the presence of the rotational lines ($R \geqslant 19$) of the 2–0 band and ($R \leqslant 9$) of the 1–0 band with almost all the rotational lines of the 4–1 band. Such an overall pattern of absorption results in a structure very sensitive to temperature. No comparison is possible between the experimental and theoretical cross-sections for the continuum or for the line wings below 2×10^{-23} cm^2. It can be seen that the Herzberg continuum could be measured at low temperature between 50,100 and 50,300 cm^{-1}. Finally, it is pointed out that the 50,000–50,500 cm^{-1} interval depends strongly on temperature; hence, the averaged absorption cross-section is related to the behaviour of the 4–1 band with the predissociation line width of its rotational lines.

8.4. *The spectral interval* 50,500–51,000 *cm*$^{-1}$

Absolute experimental and theoretical absorption cross-sections in this interval correspond mainly to the 2–0 and 5–1 bands. Again the experimental structure for absorption less than 2×10^{-23} cm^2 arises from laboratory noise. The effect of the underlying continuum is still important in the region of the 2–0 band; it is easily detected, for example, between 50,500 and 50,550 cm^{-1}. In the 50,750–51,000 cm^{-1} interval corresponding to the 5–1 band ($P3$–$P17$) the temperature effect is extremely important. It should be pointed out that the absorption cross-section of the Herzberg continuum could be measured at low temperature between 50,750 and 50,850 cm^{-1}, i.e. near 197 nm. In that interval, where the window region between the rotational lines of the 5–1 band reaches 2×10^{-23} cm^2 at 190 K, there is, therefore, a notable difference and the absorption cross-section is dependent on the Herzberg continuum, and cannot be less than 5×10^{-24} cm^2.

8.5. *The spectral interval* 51,000–51,500 *cm*$^{-1}$

In this interval where the line widths of the rotational lines of the 3–0 band play an increasing role in the overall pattern of absorption, the accuracy required for the underlying continuum is less critical than in the region of wavenumbers less than 51,000 cm^{-1}. It is clear that the wings of many lines give a detectable contribution to the effective absorption cross-section of the whole interval. Nevertheless, the role of the underlying continuum is far from negligible. Between 51,350 and 51,500 cm^{-1} the importance of the 6–1 band is dependent on its variation with temperature and on the increasing relative importance of the Herzberg continuum with decreasing temperature. The mean absorption cross-section at 190 K near 51,400–51,500 cm^{-1} is of the order of 10^{-23} cm^2 where the pseudocontinuum between the $P13$–$R15$ and $P11$–$R13$ lines of the 6–1 band is only 2×10^{-24} cm^2 near 51,450 cm^{-1}.

8.6. *The spectral interval* 51,500–52,000 *cm*$^{-1}$

This spectral region corresponds to the 4–0 band and also to portions of the 7–1 and 6–1 bands. The role of the Herzberg continuum is practically almost negligible between 52,000 and 51,750 cm^{-1} where the wings of the rotational lines contribute to the total absorption cross-section. Between 51,750 and 51,500 cm^{-1} for the ($R \geqslant 19$) lines of the 4–0 band and the first rotational lines of the 6–1 band, the variation with temperature must still be compared with an effect from the Herzberg continuum. For example, at 51,750 cm^{-1} if $T = 190$ K, the effective continuum, of the order of 10^{-23} cm^2 between the $P21$ and $P23$ lines of the 4–0 band, is associated with a pseudocontinuum of 3×10^{-24} cm^2 and corresponds to the wings of these two lines. At $T = 270$ K, the pseudocontinuum corresponds to an equivalent cross-section of about 7×10^{-23} cm^2, because the rotational population increases with temperature.

8.7. *The spectral interval* 52,000–52,500 *cm*$^{-1}$

The differences with and without an underlying continuum are small, practically negligible, in the spectral range 52,500–52,250 cm^{-1} that corresponds mainly to the $P9$–$R11$, ..., $P19$–$R21$ rotational lines of the 5–0 band with a mean predissociation line width of 2 cm^{-1}. Since the wings of the lines contribute to the absorption with a pseudocontinuum of about 10^{-22} cm^2 at 300 K, an underlying continuum even of the order of 7×10^{-24} cm^2 cannot play a consequential role. But in the spectral region corresponding to the 52,100–52,250 cm^{-1} interval, where the minimum cross-sections at 300 K reach 2×10^{-23} cm^2 between the peaks of the $P21$–$R23$ and $P25$–$R27$ lines of the 5–0 band, the contribution of the Herzberg continuum to the absorption cross-section, especially

at low temperature, is not negligible. On the other hand, in the same spectral region, the effect of temperature on the rotational structure is particularly significant because it corresponds to the lines of the 7–1 band and to the last rotational lines of the 5–0 band.

8.8. *The spectral interval* 52,500–53,000 cm^{-1}

Within this interval there is an addition of rotational lines belonging to various bands: the 6–0 band with $P \geqslant 13$, the 5–0 band with $R \leqslant 9$, the 9–1 band with $P \leqslant 9$ and the 8–1 band with $R \leqslant 1$–$R \leqslant 11$. The Herzberg continuum plays a minor or negligible role because the minimum absorption cross-sections seem to coincide with a pseudocontinuum associated with a normal contribution of the wings of the various lines. The variation of the absorption cross-sections of this pseudocontinuum are closely associated with the variation of temperature.

8.9. *The spectral interval* 53,000–53,500 cm^{-1}

The contributions of the 6–0 band, $R1$–$R13$, of the 7–0 band, $P15$–$P29$, of the 9–1 band, $R1$–$R9$, and of the 10–1 band, $R1$–$R25$, determine the structure of the absorption cross-sections. The variation of the averaged absorption cross-section is explained by the alteration of the vibrational and rotational structures between 300 and 170 K. An effect of the Herzberg continuum is outside the range of detection.

8.10. *The spectral interval* 53,500–54,000 cm^{-1}

The various structures that correspond to the 7–0 band ($R1$–$R15$) with the 8–0 band ($R15$——$R29$) and to the 11–1 band ($R1$–$R21$) with the 12–1 band ($R \geqslant 17$) indicate that the principal variation of the averaged absorption cross-section depends on temperature; this variation is particularly apparent in the spectral region 53,700–53,900 cm^{-1} where the minimum cross-section may vary by a factor of 10, between 10^{-22} and 10^{-21} cm^2 for $T = 190$ and 300 K, respectively.

8.11. *The spectral interval* 54,000–54,500 cm^{-1}

The two mains bands of this 500 cm^{-1} interval are the 8–0 band from $R1$–$R13$ and the 9–0 band from $R13$–$R29$. Three bands from the vibrational level $v'' = 1$ belong to the same interval, namely the 12–1 band from $R1$–$R15$, the 13–1 band from $P5$–$R23$, and the 14–1 band from $P17$–$R27$. The averaged absorption cross-section at 300 K is greater than 10^{-20} cm^2, and the variation of the structure is associated only with the rotational and vibrational populations dependent on temperature (300–170 K), particularly in the 54,150–54,350 cm^{-1} region.

8.12. *The spectral interval* 54,500–55,000 cm^{-1}

The 10–0 band ($P7$–$P23$) and the 9–0 band ($R1$–$P9$) are the two main bands of this interval, along with the addition of at least six bands starting from $v'' = 1$. The structure of the following bands has been measured and calculated: 14–1 from $R1$–$P17$, 15–1 from $R1$–$R21$, 16–1 from $R13$–$R25$, 17–1 from $R17$–$P25$, 18–1 from $P19$–$P27$ and 19–1 from $P19$–$R27$.

The variation of the absorption cross-sections at 300 K is of the order of 10^4, from about 4×10^{-22} cm^2 near 182.9 nm, corresponding to $P17$ of the 15–1 band, to 4×10^{-18} cm^2 at the peak of the $R9$–$P7$ lines of the 10–0 band near 181.8 nm, i.e. only for the 1 nm interval.

8.13. *The spectral interval* 55,000–55,500 cm^{-1}

This interval is characterized by almost all the rotational lines ($R1$–$R23$) of the 11–0 band, along with the first lines ($R1$–$R7$) of the 10–0 band, and the last lines ($P17$–$R29$) of the 12–0 band. Four bands with vibrational levels $v'' = 1$ are also present in the same spectral region. They are: the 16–1 band from $R1$–$P11$, the 17–1 band from $R1$–$P15$, the 18–1 band from $R1$–$R17$ and the 19–1 band from $R1$–$R19$.

The effect of the Schumann–Runge continuum can be detected. However, because the absorption cross-section of this continuum is related to the vibrational and rotational populations, it is a complicated function of temperature. The effect of temperature decreases from 300 to 170 K. The averaged absorption cross-section for this 500 cm^{-1} interval reaches almost 5×10^{-20} cm^2, while the minimum cross-section at 190 K is only 4×10^{-22} cm^2 between the $P19$ and $R19$ lines of the 11–0 band; the associated maximum cross-section comes to 6×10^{-19} cm^2 near 55,400 cm^{-1} at the peak of the $R7$ line of the 10–0 band.

8.14. *The spectral interval* 55,500–56,000 cm^{-1}

This spectral region is the last interval where a direct comparison can be made between the experimental and theoretical values. This comparison ends with the 12–0 band at 55,785 cm^{-1} (179.26 nm). The rotational structure of the 12–0 band in the 55,785–55,500 cm^{-1} interval corresponds to the rotational lines between $R1$ and $R17$. However, the 13–0, 14–0 and 15–0 bands also contribute in this 500 cm^{-1} interval from various portions of their rotational structure. The 13–0 band makes an important contribution from rotational lines between $P9$ and $R25$, but the experimental data only begin at $P17$. The 14–0 band with rotational lines between $R19$ and $R29$ has only been measured in the laboratory between $P25$ and $R29$. The 15–0 band with its lines between $P23$ and $R29$ is practically beyond the present detailed laboratory measurements.

This spectral interval has a distinctive peculiarity: the absence of rotational lines from the vibrational level $v'' = 1$, since the calculation ended with 19–1 in the preceding interval near 55,468 cm^{-1} at the rotational line $R1$.

The temperature effect is the result of the combination of a variation due to the Schumann–Runge continuum (increase with temperature) and a variation related to the rotational structure of various bands. The averaged absorption cross-section in this 500 cm^{-1} interval reaches 7×10^{-20} cm^2 at 300 K, and the extreme low and high values are 10^{-21} and 10^{-18} cm^2, respectively.

8.15. *The spectral interval* 56,000–56,500 cm^{-1}

Seven bands lie in this interval, namely the 13–0 band from $R1$–$P7$, the 14–0 band from $R1$–$P17$, the 15–0 band from $R7$–$R23$, the 16–0 band from $R15$–$P25$, the 17–0 band from $P17$–$R27$, the 18–0 band from $P19$–$P27$ and the 19–0 band from $P21$–$P27$.

Among all these bands the 14–0 and 15–0 bands are most important in this 500 cm^{-1} interval where the averaged absorption cross-section is greater than 10^{-19} cm^2. It is expected that the individual structures of all the components cannot be very accurate, but the number of possible errors due to various causes does not permit classification of all the uncertainities.

8.16. *The spectral interval* 56,500–57,000 cm^{-1}

In this last 500 cm^{-1} interval illustrated in our atlas we must consider at least all the first rotational lines of the 15–0 to 19–0 bands, namely 15–0 from $R1$–$R7$, 16–0 from $R1$–$P13$, 17–0 from $R1$–$R17$, 18–0 from $R1$–$P19$, and 19–0 from $P3$–$P19$. The effect of the Schumann–Runge continuum must be introduced into the calculation with its temperature dependence.

Because of various uncertainties, detailed characterization of the theoretical results is difficult. The adopted equivalent line widths depend essentially on the analysis of rotational lines from vibrational levels $v'' = 1$ which may be equivocal. The total uncertainty which is difficult to quantify could perhaps reach several tens of per cent.

9. AERONOMIC PARAMETERS FOR THE SCHUMANN–RUNGE BANDS

The various parameters to be used for the calculation of the O_2 transmittance and its photodissociation frequency for the 16 spectral intervals of 500 cm^{-1} described in Section 8 are given in Table 4, where the individual absorption cross-sections are listed and where the solar irradiances deduced from the SUSIM observations (see Nicolet and Kennes, 1988) are used to determine the photodissociation frequencies at optical depth, $\tau_{O_2} = 0$.

Because the O_2 cross-sections presented in Table 4 for various temperature intervals are averaged values over the 500 cm^{-1} spectral ranges at zero optical depth, they coincide with the maximum cross-sections defined by $N(O_2) = 0$. In order to give an idea of the variations in the O_2 absorption Table 5 gives the mean cross-sections, the corresponding number of O_2 absorbing molecules $N(cm^{-1})$ and the appropriate altitudes z (km) for the optical depths $\tau = 0.1$, 1.0 and 10. From this table it is possible to decide the best approach to arrive at correct estimates of the beginning of the absorption ($\tau = 0.1$), to the approximate

TABLE 4. ABSORPTION CROSS-SECTIONS (cm^2) AND NUMBER OF PHOTONS ($cm^{-2}\ s^{-1}/500\ cm^{-1}$) AT ZERO OPTICAL DEPTH

Number	Interval (cm^{-1})	Cross-section	Temperature (K)	Herzberg continuum	O_3 cross-sections	Number of photons
1	49000–49500	$7.90 \pm 0.05 \times 10^{-24}$	$170 \leqslant T \leqslant 270$	7.2×10^{-24}	3.26×10^{-19}	1.92×10^{12}
2	49500–50000	$1.05 \pm 0.07 \times 10^{-23}$	$170 \leqslant T \leqslant 270$	7.4×10^{-24}	3.14×10^{-19}	1.69×10^{12}
3	50000–50500	$1.34 \pm 0.15 \times 10^{-23}$	$200 \leqslant T \leqslant 270$	7.5×10^{-24}	3.30×10^{-19}	1.38×10^{12}
4	50500–51000	$4.22 \pm 0.25 \times 10^{-23}$	$170 \leqslant T \leqslant 270$	7.5×10^{-24}	3.69×10^{-19}	1.29×10^{12}
5	51000–51500	$1.55 \pm 0.05 \times 10^{-22}$	$170 \leqslant T \leqslant 270$	7.5×10^{-24}	4.11×10^{-19}	1.14×10^{12}
6	51500–52000	$4.83 \pm 0.07 \times 10^{-22}$	$210 \leqslant T \leqslant 270$	7.4×10^{-24}	4.38×10^{-19}	7.81×10^{11}
7	52000–52500	$6.33 \pm 0.33 \times 10^{-22}$	$210 \leqslant T \leqslant 270$	7.2×10^{-24}	4.80×10^{-19}	8.07×10^{11}
8	52500–53000	$1.34 \pm 0.07 \times 10^{-21}$	$210 \leqslant T \leqslant 270$	7.0×10^{-24}	5.31×10^{-19}	6.89×10^{11}
9	53000–53500	$3.06 \pm 0.15 \times 10^{-21}$	$180 \leqslant T \leqslant 270$	6.7×10^{-24}	5.88×10^{-19}	5.98×10^{11}
10	53500–54000	$7.04 \pm 0.40 \times 10^{-21}$	$180 \leqslant T \leqslant 270$	6.4×10^{-24}	6.40×10^{-19}	4.81×10^{11}
11	54000–54500	$1.34 \pm 0.07 \times 10^{-20}$	$180 \leqslant T \leqslant 270$	6.0×10^{-24}	6.88×10^{-19}	4.04×10^{11}
12	54500–55000	$2.92 \pm 0.10 \times 10^{-20}$	$170 \leqslant T \leqslant 290$	5.6×10^{-24}	7.29×10^{-19}	4.12×10^{11}
13	55000–55500	$4.63 \pm 0.03 \times 10^{-20}$	$180 \leqslant T \leqslant 270$		7.63×10^{-19}	3.72×10^{11}
14	55500–56000	$6.24 \pm 0.25 \times 10^{-20}$	$180 \leqslant T \leqslant 250$		7.86×10^{-19}	2.82×10^{11}
15	56000–56500	$1.12 \pm 0.02 \times 10^{-19}$	$180 \leqslant T \leqslant 230$		7.99×10^{-19}	2.55×10^{11}
16	56500–57000	$1.65 \pm 0.01 \times 10^{-19}$	$170 \leqslant T \leqslant 250$		8.11×10^{-19}	2.01×10^{11}

TABLE 5. AERONOMIC PARAMETERS FOR 500 cm^{-1} INTERVALS

49500 - 49000 cm^{-1} (0-0,2-1)				50000 - 49500 cm^{-1} (1-0,3-1)		
τ	0.1	1.0	10	0.1	1.0	10
σ (cm^2)	7.8×10^{-24}	7.5×10^{-24}	7.5×10^{-24}	1.0×10^{-23}	8.75×10^{-24}	8.0×10^{-24}
N (cm^{-2})	1.3×10^{22}	1.3×10^{23}	1.3×10^{24}	1.0×10^{22}	1.15×10^{23}	1.25×10^{24}
z (km)	50	25	15	50	25	15
50500 - 50000 cm^{-1} (1-0,2-0)				51000 - 50500 cm^{-1} (2-0,5-1)		
σ	1.3×10^{-23}	1.0×10^{-23}	8.0×10^{-24}	2.5×10^{-23}	1.4×10^{-23}	8.0×10^{-24}
N	8×10^{21}	1.0×10^{23}	1.25×10^{24}	4×10^{21}	7×10^{22}	1.2×10^{24}
z	50	30	15	60	30	15
51500-51000 cm^{-1} (3-0,6-1)				52000-51500 cm^{-1} (4-0,6-1,7-1)		
σ	1×10^{-22}	3×10^{-23}	1×10^{-23}	3×10^{-22}	1×10^{-22}	1.5×10^{-23}
N	1×10^{21}	3×10^{22}	1×10^{24}	3.5×10^{20}	1×10^{22}	7×10^{23}
z	65	35	15	70	45	20
52500-52000 cm^{-1} (5-0,7-1,8-1)				53000-52500 cm^{-1} (6-0,5-0,9-1,8-1)		
σ	2×10^{-22}	7.5×10^{-23}	2×10^{-23}	6.5×10^{-22}	1.2×10^{-22}	3×10^{-23}
N	5×10^{20}	1.3×10^{22}	5×10^{23}	1.5×10^{20}	7×10^{21}	3×10^{23}
z	70	45	20	75	50	25
53500-53000 cm^{-1} (6-0,7-0,9-1,10-1)				54000-53500 cm^{-1} (7-0,8-0,11-1)		
σ	1.5×10^{-21}	3×10^{-22}	6×10^{-23}	5×10^{-21}	1×10^{-21}	1.75×10^{-22}
N	6×10^{19}	3×10^{21}	1.5×10^{23}	2×10^{19}	1×10^{21}	6×10^{22}
z	80	55	35	85	60	35
54500-54000 cm^{-1} (8-0,9-0)				55000-54500 cm^{-1} (10-0,9-0)		
σ	12×10^{-20}	1×10^{-21}	2.5×10^{-22}	2×10^{-20}	2×10^{-21}	5×10^{-22}
N	1×10^{19}	1×10^{21}	4×10^{22}	5×10^{18}	5×10^{20}	2×10^{22}
z	90	65	35	95	70	40
55500-55000 cm^{-1} (11-0)				56000-55500 cm^{-1} (12-0,13-0)		
σ	3.5×10^{-20}	5×10^{-21}	1×10^{-21}	5×10^{-20}	7×10^{-21}	2×10^{-21}
N	3×10^{18}	2×10^{20}	10^{22}	2×10^{18}	1.5×10^{20}	5×10^{21}
z	100	75	45	100	75	55
56500-56000 cm^{-1} (15-0,14-0)				57000-56500 cm^{-1} (19-0 to 15-0)		
σ	1×10^{-19}	2×10^{-20}	5×10^{-21}	1.6×10^{-19}	8×10^{-20}	2×10^{-20}
N	1×10^{18}	5×10^{19}	2×10^{21}	$< 10^{18}$	1.3×10^{19}	5×10^{20}
z	100	80	60	> 100	90	70

maximum of the absorption ($\tau = 1.0$) and of the minimum value of the absorption cross-section ($\tau = 10$) that corresponds to a negligible transmittance of the order of 5×10^{-5}. The altitudes associated with the different optical depths indicate clearly what the atmospheric regions are that correspond to the principal behavior for each 500 cm^{-1} interval between 57,000 and 49,000 cm^{-1}. For example, the interval between 49,000 and 49,500 cm^{-1} that corresponds to the 0–0 and 2–1 bands has an absorption cross-section practically identical to that of the Herzberg continuum, about 7.5×10^{-24} cm^2

The spectral range between 49,500 and 53,000 cm^{-1} is typically representative of the stratosphere while the spectral region between 54,000 and 56,000 cm^{-1} is particularly associated with the mesosphere. The 500 cm^{-1} interval between 56,500 and 57,000 cm^{-1} that corresponds to the spectral range of the 19–0 to 16–0 bands plays a role in the lower thermosphere.

It may be added that there is no practical rule that may be used to derive the decrease of the averaged absorption cross-section between the optical depths $\tau = 0.1$–10. The superposition of bands from $v'' = 0$ to 1 dependent on the effect of temperature with height is different for each 500 cm^{-1} interval. A detailed parameterization is required.

10. PHOTODISSOCIATION IN THE MESOSPHERE

The photodissociation frequency (s^{-1}) and the photodissociation rate (cm^{-3} s^{-1}) for the Herzberg continuum have been obtained for various atmospheric conditions (Nicolet and Kennes, 1988). But the atomic oxygen production in the spectral interval of the predissociation bands of the Schumann–Runge system is a different problem. Nevertheless, when the atmospheric opacity from ozone absorption and molecular scattering is negligible, it is possible to determine the total photodissociation frequency and photodissociation rate if the solar irradiance is known. With the SUSIM data given in Table 5 we can determine the oxygen production.

Above the mesopause, the photodissociation frequency is $J(O_2)_{SRB} = 1.25 \times 10^{-7}$ s^{-1} for the Schumann–Runge bands (57,000–49,500 cm^{-1}) and $J(O_2)_{HER} = 5.8 \times 10^{-10}$ s^{-1} for the Herzberg continuum (49,500–41,250 cm^{-1}). The atmospheric optical depth $\tau_A = 0$, the molecular scattering optical depth $\tau_{MS} = 0$, and the O_3 optical depth $\tau_{O_3} = 0$.

The effect of the O_3 absorption on the transmittance, and therefore on $J(O_2)_{SRB}$ is negligible or relatively small in the mesosphere. From 60 to 50 km, the effect of ozone is to decrease the photodissociation frequency, $10^{-10} < J(O_2)_{SRB} < 10^{-9}$ s^{-1}, from 0.02×10^{-10} s^{-1} to 0.04×10^{-10} s^{-1}, respectively, i.e. less than 4%. Thus, the adoption of a general formula from the mesopause to the stratopause can be envisaged for $J(O_2)_{SRB}$. The result is (Fig. 1)

$$J(O_2)_{SRB} = 6.55 \times 10^6 N^{-0.7567}\ s^{-1}$$

for

$$5 \times 10^{18} \leqslant N(O_2) \leqslant 1 \times 10^{22}\ cm^{-2}$$

i.e. up to 95 and down to 50 km near $N = 10^{22}$ cm^{-2}, with an accuracy generally better than $\pm 5\%$ and

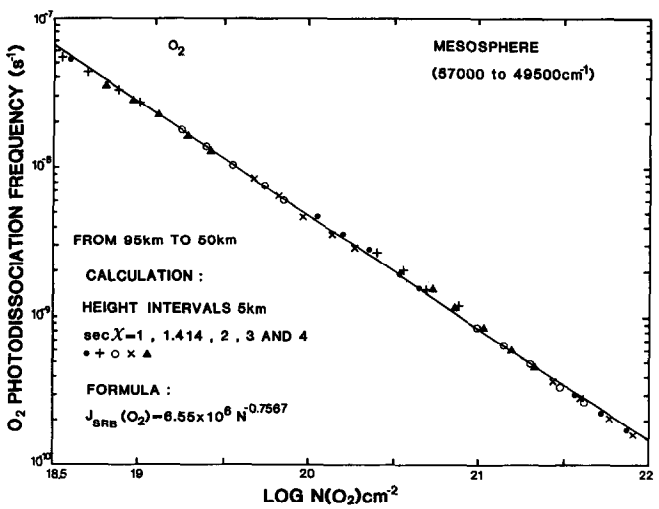

FIG. 1. PHOTODISSOCIATION FREQUENCY OF O_2 IN THE MESOSPHERE FOR THE SPECTRAL INTERVAL 175–202 nm THAT CORRESPONDS TO THE SCHUMANN–RUNGE BAND PREDISSOCIATION.

always better than $\pm 10\%$. Such a result corresponds to

$$5 \times 10^{-8} \geqslant J(O_2)_{SRB} \geqslant 5 \times 10^{-10} s^{-1}.$$

If the reference solar irradiance published in WMO (1985) is adopted the preceding formula (Nicolet, 1987) becomes

$$J(O_2)_{SRB} = 3 \times 10^{-7} N^{-0.795} s^{-1}$$

and the numerical results indicate a decrease of $J(O_2)$ of 15, 25, 40 and 50% at $N(O_2) = 10^{19}$, 10^{20}, 10^{21} and 10^{22} cm^{-2}, respectively. Thus, the precision in the solar irradiance values should be improved.

The addition of the photodissociation produced in the Herzberg continuum increases the total photodissociation at 95 km by 1–2% and at 90 km by 2–4%.

At the mesopause, the contribution to the total photodissociation of O_2 by the Herzberg continuum increases from (Fig. 2)

3% for $\sec\chi = 1$ and $N(O_2) = 1.8 \times 10^{19}$ cm^{-2}

to

9% for $\sec\chi = 4$ and $N(O_2) = 7.1 \times 10^{19}$ cm^{-2}.

In the region of 60–65 km, the role of the Herzberg continuum in the total production of atomic oxygen increases up to more than 50% when $N(O_2) = 2 \times 10^{21}$ cm^{-2}. The following table provides the details of the calculation at 60 km for $\sec\chi = 1$, 1.414, 2, 3 and 4, respectively.

$N(O_2)$	$J(O_2)$	% Herzberg	$n(O_2)J(O_2)$
1×10^{21}	1.4×10^{-9}	40	1.9×10^{6}
1.4×10^{21}	1.2×10^{-9}	47	1.6×10^{6}
2×10^{21}	1.1×10^{-9}	54	1.4×10^{6}
3×10^{21}	9.0×10^{-10}	62	1.2×10^{6}
4×10^{21}	8.2×10^{-10}	67	1.1×10^{6}

Consequently, the atomic oxygen production therefore lies between 4 and 2×10^{6} atoms cm^{-3} s^{-1} for solar zenith angles between 0° and 70° (Fig. 3).

The stratospheric conditions were described by Nicolet and Kennes (1988) between 55 and 15 km.

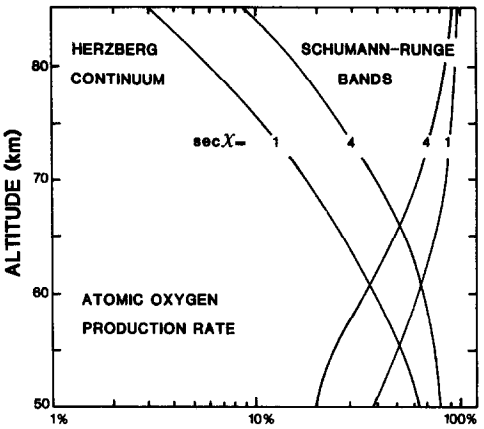

FIG. 2. RELATIVE PRODUCTION RATE OF OXYGEN ATOMS BY DIRECT PHOTODISSOCIATION OF O_2 IN THE SPECTRAL RANGES OF THE SCHUMANN–RUNGE BANDS AND OF THE HERZBERG CONTINUUM BETWEEN 85 AND 50 km.

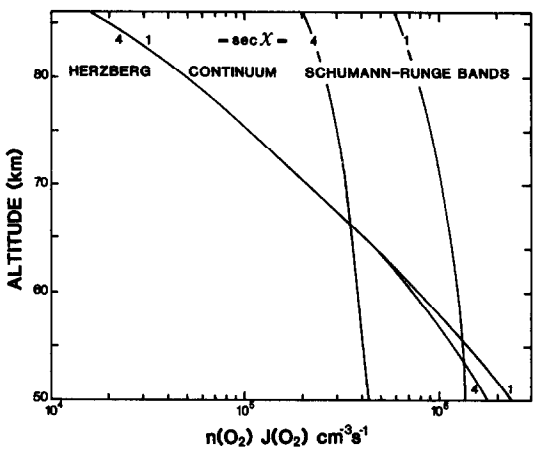

FIG. 3. PHOTODISSOCIATION RATES OF O_2 (cm^{-3} s^{-1}) IN THE MESOSPHERE FOR TWO SOLAR ZENITH ANGLES: $\sec\chi = 1$ AND 4. Comparison between the effects of the Herzberg continuum and of the photodissociation of the Schumann–Runge bands.

11. CONCLUDING REMARK

The combination of high resolution absorption cross-section measurements with a parallel theoretical calculation adapted to the atmospheric conditions provide the means of determining the molecular oxygen photodissociation in the spectral range of the Schumann–Runge region with excellent accuracy. The parameterization of the O_2 transmittance and of the photodissociation frequency will be given in a subsequent paper.

Acknowledgements—Support for the preparation of this paper has been provided by the Chemical Manufacturers Association, Contract FC 85-563 with the Institut d'Aéronomie Spatiale, by the Commission of the European Communities, Directorate-General for Science, Research and Development, Environment Research Programme, and by the Office of Naval Research contract with the Communications and Space Sciences Laboratory of the Penn State University.

REFERENCES

Ackerman, M. and Biaumé, F. (1970) Structure of the Schumann–Runge bands from the (0–0) to the (13–0) band. *J. molec. Spectrosc.* **35**, 73.

Ackerman, M., Biaumé, F. and Kockarts, G. (1970) Absorption cross-sections of the Schumann–Runge bands of molecular oxygen. *Planet. Space Sci.* **18**, 1639.

Ackerman, M., Biaumé, F. and Nicolet, M. (1969). Absorption in the spectral range of the Schumann–Runge bands. *Can. J. Chem.* **47**, 1834.

Allen, M. and Frederick, J. E. (1982) Effective photodissociation cross-sections for molecular oxygen and nitric oxide in the Schumann–Runge bands. *J. atmos. Sci.* **39**, 2066.

Allison, A. C., Dalgarno, A. and Pasachoff, N. W. (1971) Absorption by vibrationally excited molecular oxygen in the Schumann–Runge continuum. *Planet. Space Sci.* **19**, 1463.

Anderson, G. P. and Hall, L. A. (1986) Stratospheric determination of O_2 cross sections and photodissociation rate coefficients: 191–215 nm. *J. geophys Res.* **91**, 14509.

Biaumé, F. (1972a) Détermination de la valeur absolue de l'absorption dans les bandes du système de Schumann–Runge de l'oxygène moléculaire. *Aeron. Acta Brussels* A No. 100, 270 pp.

Biaumé, F. (1972b) Structure de rotation des bandes (0–0) à (13–0) du système de Schumann–Runge de la molécule d'oxygène. *Acad. R. Belg. Mém. Cl. Sci.* **40**, 66.

Blake, A. J. (1979) An atmospheric absorption model for the Schumann–Runge bands of oxygen. *J. geophys. Res.* **84**, 3272.

Brix, P. and Herzberg, G. (1954) Fine structure of the Schumann–Runge bands near the convergence limit and the dissociation energy of oxygen molecule. *Can. J. Phys.* **32**, 110.

Cheung, A. S.-C., Yoshino, K., Parkinson, W. H. and Freeman, D. E. (1986) Molecular spectroscopic constants of O_2 ($^3\Sigma_u^-$), the upper state of the Schumann–Runge bands. *J. molec. Spectrosc.* **119**, 1.

Cheung, A. S.-C., Yoshino, K., Parkinson, W. R., Guberman, S. L. and Freeman, D. E. (1986) Absorption cross-section measurements of oxygen in the wavelength region 195–241 nm of the Herzberg continuum. *Planet. Space Sci.* **34**, 1007.

Ditchburn, R. W. and Young, P. A. (1962) The absorption of molecular oxygen between 1850 and 2500 Å. *J. atmos. terr. Phys.* **24**, 127.

Fang, T. M., Wofsy, S. C. and Dalgarno, A. (1974). Opacity distribution functions and absorption in Schumann–Runge bands of molecular oxygen. *Planet. Space Sci.* **22**, 413.

Frederick, J. E. and Hudson, R. D. (1979) Predissociation linewidths and oscillator strengths for the 2–0 to 13–0 Schumann–Runge bands of O_2. *J. molec. Spectrosc.* **74**, 247.

Frederick, J. E. and Hudson, R. D. (1980a) Dissociation of molecular oxygen in the Schumann–Runge Bands. *J. atmos. Sci.* **37**, 1099.

Frederick, J. E. and Hudson, R. D. (1980b) Atmospheric opacity in the Schumann–Runge bands and the aeronomic dissociation of water vapor. *J. atmos. Sci.* **37**, 1088.

Frederick, J. E. and Mentall, J. E. (1982) Solar irradiance in the stratosphere: implications for the Herzberg continuum absorption of O_2. *Geophys. Res. Lett.* **9**, 461.

Gibson, S. T., Gies, H. P. F., Blake, A. J. and McCoy, D. G. (1983a) Transmittance of the atmosphere in the (8–0) and (9–0) Schumann–Runge bands of oxygen. *J. geophys. Res.* **83**, 500.

Gibson, S. T., Gies, H. P. F., Blake, A. J., McCoy, D. G. and Rogers, P. J. (1983b) Temperature dependence in the Schumann–Runge photoabsorption continuum of oxygen. *J. quant. Spectrosc. radiat. Transfer* **30**, 385.

Gies, H. P. F., Gibson, S. T., McCoy, D. G., Blake, A. J. and Lewis, B. R. (1981) Experimentally determined oscillator strengths and line widths for the Schumann–Runge band system of molecular oxygen—III. The (7–0)–(19–0) Bands. *J. quant. Spectrosc. radiat. Transfer* **26**, 469.

Gies, H. P. F., Gibson, S. T., Blake, A. J. and McCoy, D. G. (1982). The Schumann–Runge continuum of oxygen at wavelengths greater than 175 nm. *J. geophys. Res.* **87**, 8307.

Hasson, V. and Nicholls, R. W. (1971) Absolute spectral absorption measurements on molecular oxygen from 2640–1920 Å: II Continuum measurements 2430–1920 Å. *J. Phys. B: Atomic Molec. Phys.* **4**, 1789.

Herman, J. R. and Mentall, J. E. (1982) O_2 absorption cross sections (187–225 nm) from stratospheric solar flux measurements. *J. geophys. Res.* **87**, 8967.

Hudson, R. D. and Carter, V. L. (1969) Absorption in the spectral range of the Schumann–Runge bands. *Can. J. Chem.* **47**, 1840.

Hudson, R. D., Carter, V. L. and Breig, E. L. (1969) Predissociation in the Schumann–Runge band system of O_2: laboratory measurements and atmospheric effects. *J. geophys. Res.* **74**, 4079.

Hudson, R. D. and Mahle, S. H. (1972) Photodissociation rates of molecular oxygen in the mesosphere and lower thermosphere. *J. geophys. Res.* **77**, 2902.

Jarmain, R. W. and Nicholls, R. W. (1967) A theoretical study of the $v'' = 0, 1, 2$ progressions of bands and adjoining photodissociation continua of the O_2 Herzberg I system. *Proc. Phys. Soc.* **90**, 545.

Jenouvrier, A., Coquart, B. and Merienne-Lafore, M. F. (1986) New measurements of the absorption cross sections in the Herzberg continuum of molecular oxygen in the region between 205 and 240 nm. *Planet. Space Sci.* **34**, 253.

Johnston, H. S., Paige, M. and Yao, F. (1984) Oxygen absorption cross sections in the Herzberg continuum and between 206 and 327 K. *J. geophys. Res.* **89**, 11661.

Kockarts, G. (1971) Penetration of solar radiation in the Schumann–Runge bands of molecular oxygen, in *Mesospheric Models and Related Experiments* (Edited by Fiocco, G.), p. 160. Reidel, Dordrecht, Holland.

Kockarts, G. (1976) Absorption and photodissociation in the Schumann–Runge bands of molecular oxygen in the terrestrial atmosphere. *Planet. Space Sci.* **24**, 589.

Lewis, B. R., Berzins, L. and Carver, J. H. (1986a) Oscillator strengths for the Schumann–Runge bands of $^{16}O_2$. *J. quant. Spectrosc. radiat. Transfer* **36**, 209.

Lewis, B. R., Berzins, L., Carver, J. H. and Gibson, S. T. (1985a) Decomposition of the photoabsorption continuum underlying the Schumann–Runge bands of $^{16}O_2$—I. Role of the $B^3\Sigma$ state. I—A new dissociation limit. *J. quant. Spectrosc. radiat. Transfer* **33**, 627.

Lewis, B. R., Berzins, L., Carver, J. H. and Gibson, S. T. (1986b) Rotational variation of predissociation linewidth in the Schumann–Runge bands of $^{16}O_2$. *J. quant. Spectrosc. radiat. Transfer* **36**, 187.

Lewis, B. R., Berzins, L., Carver, J. H., Gibson, S. T. and McCoy, D. G. (1985b) Decomposition of the photo-

absorption continuum underlying the Schumann–Runge bands of $^{16}O_2$—II. Role of the $1\ ^3\pi$ state and collision induced absorption. *J. quant. Spectrosc. radiat. Transfer* **34**, 405.

Lewis, B. R., Carver, J. H., Hobbs, T. I., McCoy, D. G. and Gies, H. P. F. (1978) Experimentally determined oscillator strengths and linewidths for the Schumann–Runge band system of molecular oxygen—I. The (6–0)–(14–0) bands. *J. quant. Spectrosc. radiat. Transfer* **20**, 191.

Lewis, G. R., Carver, J. H., Hobbs, T. I., McCoy, D. G. and Gies, H. P. F. (1979) Experimentally determined oscillator strengths and linewidths for the Schumann–Runge band system of molecular oxygen, II. The (2–0) to (5–0) bands. *J. quant. Spectrosc. radiat. Transfer* **21**, 213.

Lewis, B., Carver, J. H., Hobbs, T. L., McCoy, D. G. and Gies, H. P. F. (1980) Rotational variation of predissociation linewidths for the Schumann–Runge bands of molecular oxygen. *J. quant. Spectrosc. radiat. Transfer* **24**, 365.

Lewis, B. R., Carver, J. H., Hobbs, T. I., McCoy, D. G. and Gies, H. P. F. (1986c) Rotational variation of predissociation linewidths for the Schumann–Runge bands of molecular oxygen. *J. quant. Spectrosc. radiat. Transfer* **24**, 365.

Miller, S. L. and Townes, C. H. (1953). The microwave spectrum of ($^{16}O_2$) and $^{16}O^{17}O$. *Phys. Rev.* **90**, 537.

Nicolet, M. (1979) Etude des réactions chimiques de l'ozone dans la stratosphère. Institut Royal Météorologique, Bruxelles, 536 pp.

Nicolet, M. (1981) The solar spectral irradiance and its action in the atmospheric photodissociation processes. *Planet. Space Sci.* **29**, 951.

Nicolet, M. (1983) The influence of solar radiation on atmospheric chemistry. *Ann. Géophys.* **1**, 493.

Nicolet, M. (1985) Aeronomical aspects of mesospheric photodissociation: processes resulting from the H-Lyman-alpha line. *Planet. Space Sci.* **33**, 69.

Nicolet, M. (1987) Spectral solar irradiances and aeronomic photolytic processes in the mesosphere, in *Recent Studies in Atomic and Molecular Processes* (Edited by Kingston, A. E.), p. 91. Plenum, New York.

Nicolet, M. and Cieslik, S. (1980) The photodissociation of nitric oxide in the mesosphere and stratosphere. *Planet. Space Sci.* **28**, 105.

Nicolet, M., Cieslik, S. and Kennes, R. (1987) Rotational structure and absorption cross-sections from 300 to 190 K of the Schumann–Runge bands. *Aeronomica Acta* A No. 318, 340 pp.

Nicolet, M., Cieslik, S. and Kennes, R. (1988) Aeronomic problems of molecular oxygen photodissociation. II. Theoretical absorption cross-sections of the Schumann–Runge bands at 79 K. *Planet. Space Sci.* **36**, 1039.

Nicolet, M. and Kennes, R. (1986) Aeronomic problems of molecular oxygen photodissociation. I. The O_2 Herzberg continuum. *Planet. Space Sci.* **34**, 1043.

Nicolet M. and Kennes, R. (1988) Aeronomic problems of molecular oxygen photodissociation—III. Solar spectral irradiances in the region of the O_2 Herzberg continuum, Schumann–Runge bands and continuum. *Planet. Space Sci.* **36**, 1059.

Nicolet, M. and Mange, P. (1954) The dissociation of oxygen in the high atmosphere. *J. geophys. Res.* **59**, 15.

Nicolet, M. and Peetermans, W. (1980). Atmospheric absorption in the O_2 Schumann–Runge bands spectral range and photodissociation rates in the stratosphere and mesosphere. *Planet. Space Sci.* **28**, 85.

Ogawa, M. (1971) Absorption cross-sections of O_2 and CO_2 continua in the Schumann- and far UV regions. *J. chem. Phys.* **54**, 2550.

Saxon, R. P. and Slanger, R. P. (1986) Molecular oxygen absorption continua at 200–300 and O_2 radiative lifetimes. *J. geophys. Res.* **91**, 9877.

Shardanand and Prasad Rao, A. D. (1977) Collisons induced absorption of O_2 in the Herzberg continuum. *J. quant. Spectrosc. radiat. Transfer* **17**, 433.

Tatum, J. B. and Watson, J. K. G. (1971) Rotational line strength in $3\Sigma^+$–$3\Sigma^+$ transitions with intermediate coupling. *Can. J. Phys.* **49**, 2693.

Whiting, A. (1968) An empirical approximation to the Voigt profile. *J. quant. Spectrosc. radiat. Trans.* **8**, 1379.

Yoshino, K., Freeman, D. E., Esmond, J. R. and Parkinson, W. H. (1983) High resolution absorption cross-section measurements and band oscillator strengths of the (1, 0)–(12, 0) Schumann–Runge bands of O_2. *Planet. Space Sci.* **31**, 339.

Yoshino, K., Freeman, J. R., Esmond, J. R. and Parkinson, W. H. (1987) High resolution absorption cross-sections and band oscillator strengths of the Schumann–Runge bands of oxygen at 79 K. *Planet. Space Sci.* **35**, 1067.

Yoshino, K., Freeman, D. E. and Parkinson, W. H. (1984) Atlas of the Schumann–Runge absorption bands of O_2 in the wavelength region 175–205 nm. *J. phys. Chem. (Ref. Data)* **13**, 207.

APPENDIX—ABSORPTION CROSS-SECTIONS

Summary

Figures of calculated and experimental absorption cross-sections are given for molecular oxygen as a function of wavenumber over the spectral interval 49,000–57,000 cm^{-1} at 300 K. The spectrum corresponds to the domain of the rotational lines of the various bands of the $B\ ^3\Sigma_u^- - X\ ^3\Sigma_g^-$ Schumann–Runge system with their underlying continua; it is presented for the range of the 0–0 to 19–0 bands in 32 intervals of 250 cm^{-1}. Calculated absorption cross-sections have been determined for each band after comparison with the most recent laboratory measurements made at 300 K. The calculations required knowledge of the line wavenumbers of the 0–0 to 19–0 and 2–1 to 19–1 bands with their mean oscillator strengths and determination of the associated equivalent line widths of the rotation lines with their underlying continuum.

Basic data

Figures A1–A32 are intended to serve those who require detailed information about the ultraviolet absorption of molecular oxygen in the predissociation region of the O_2 Schumann–Runge system. This inventory makes use of the recent experimental data on the rotational lines and underlying continua after analysis of the extensive literature on oxygen absorption coefficients.

After the first detailed analyses, such as those determining wavelength assignments, for $v' \geqslant 12$, of Brix and Herzberg (1954) and, for $v' \leqslant 13$, of Ackerman and Biaumé (1970) and Biaumé (1972a,b), extensive wavenumber measurements of the rotation lines of the O_2 Schumann–Runge absorption bands were provided by Yoshino *et al.* (1984). These sets of data are also the most accurate, and are almost complete, since the cross-sections are absolute, the line widths being in excess of the instrument resolution for the various bands studied.

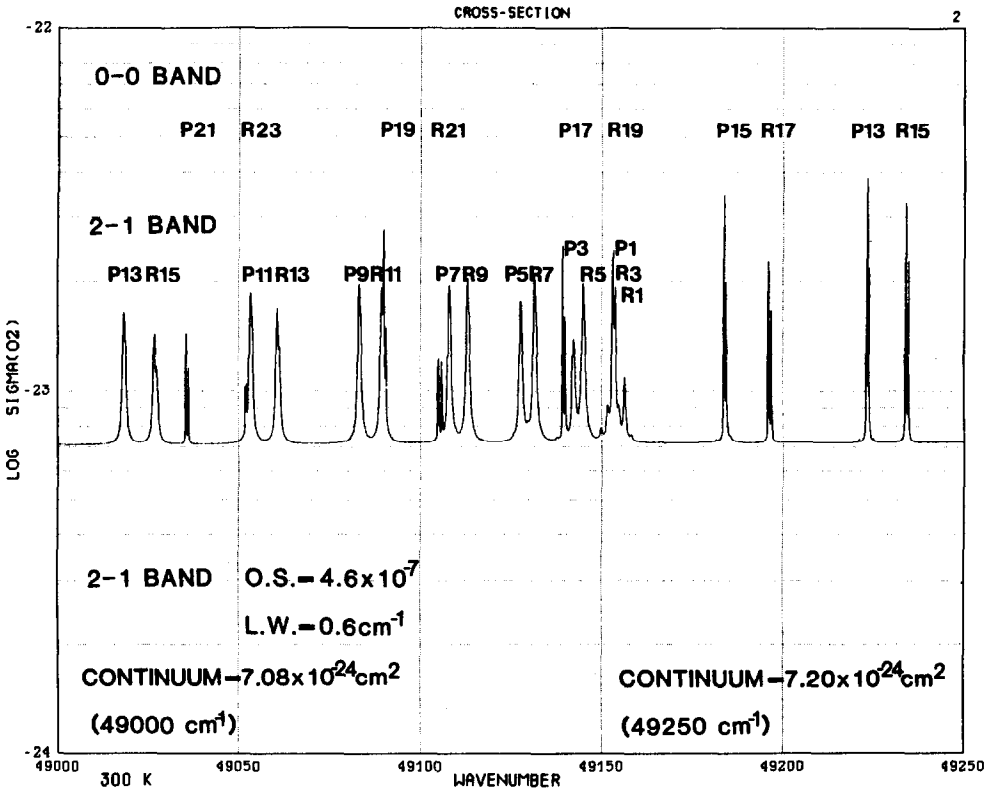
CROSS-SECTION
2
-22
-23
-24
0-0 BAND
P21 R23 P19 R21 P17 R19 P15 R17 P13 R15
2-1 BAND
P13 R15 P11 R13 P9 R11 P7 R9 P5 R7 P3 R5 P1 R3 R1
2-1 BAND O.S.=4.6x10^-7
L.W.=0.6cm^-1
CONTINUUM=7.08x10^-24cm^2
(49000 cm^-1)
CONTINUUM=7.20x10^-24cm^2
(49250 cm^-1)
LOG SIGMA(O2)
49000 49050 49100 49150 49200 49250
300 K
WAVENUMBER

FIG. A1.

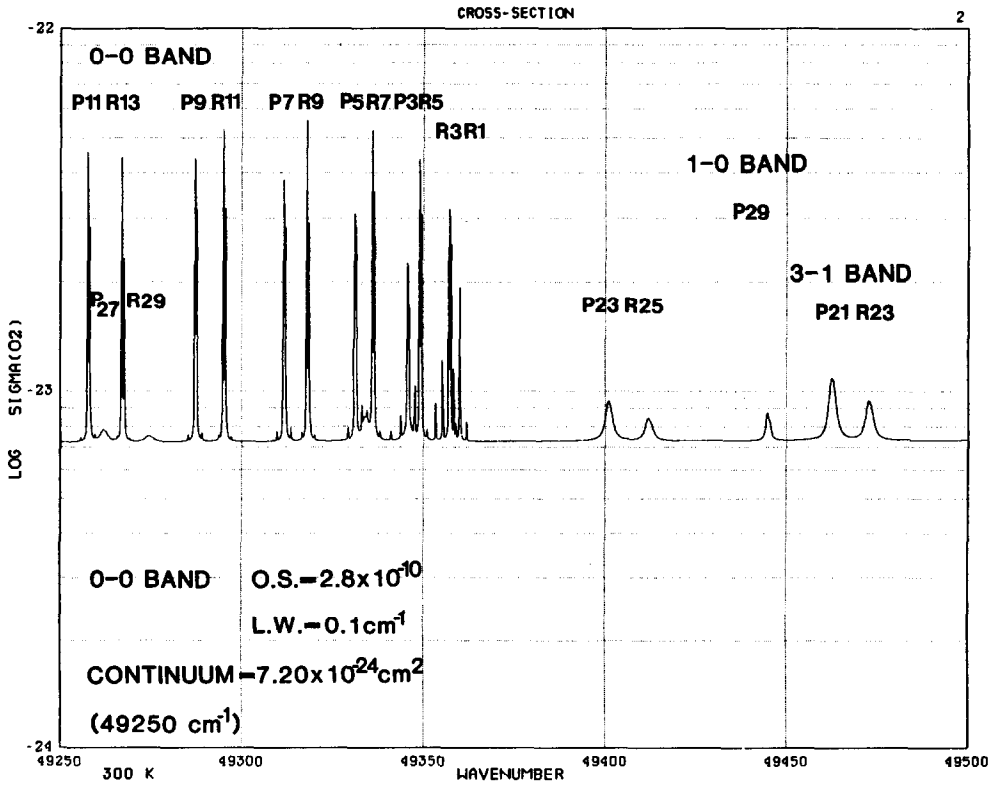
CROSS-SECTION
2
-22
-23
-24
0-0 BAND
P11 R13 P9 R11 P7 R9 P5 R7 P3 R5 R3 R1
P27 R29
1-0 BAND
P29
P23 R25
3-1 BAND
P21 R23
0-0 BAND O.S.=2.8x10^-10
L.W.=0.1cm^-1
CONTINUUM=7.20x10^-24cm^2
(49250 cm^-1)
LOG SIGMA(O2)
49250 49300 49350 49400 49450 49500
300 K
WAVENUMBER

FIG. A2.

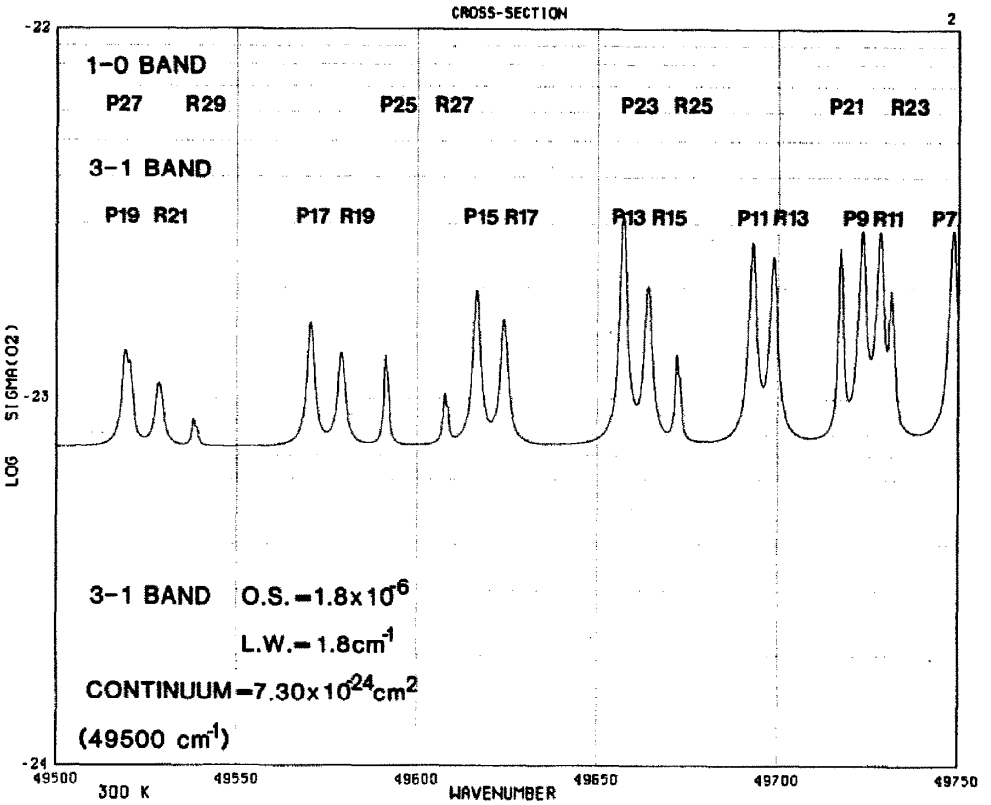
CROSS-SECTION
2
1-0 BAND
P27 R29
P25 R27
P23 R25
P21 R23
3-1 BAND
P19 R21
P17 R19
P15 R17
P13 R15
P11 R13
P9 R11
P7
LOG SIGMA(O2)
-22
-23
-24
3-1 BAND O.S.=1.8x10^-6
L.W.=1.8cm^-1
CONTINUUM=7.30x10^-24cm^2
(49500 cm^-1)
49500
300 K
49550
49600
49650
49700
49750
WAVENUMBER

FIG. A3.

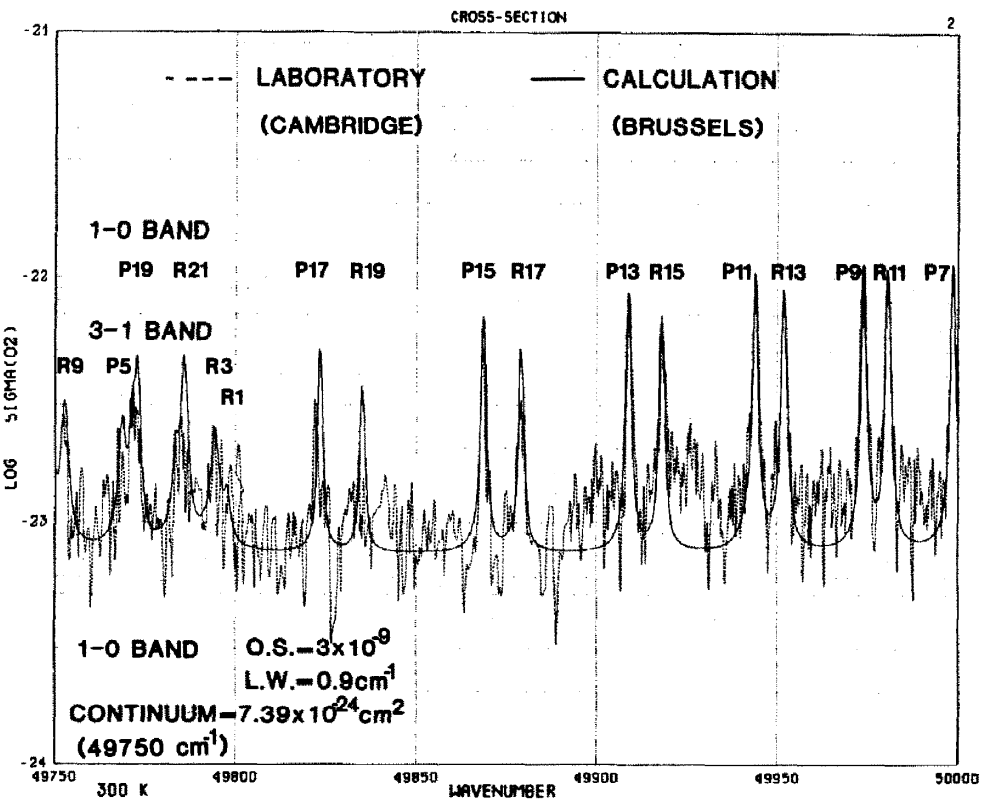
CROSS-SECTION
2
LABORATORY
(CAMBRIDGE)
CALCULATION
(BRUSSELS)
1-0 BAND
P19 R21
P17 R19
P15 R17
P13 R15
P11 R13
P9 R11
P7
3-1 BAND
R9 P5
R3
R1
LOG SIGMA(O2)
-21
-22
-23
-24
1-0 BAND O.S.=3x10^-9
L.W.=0.9cm^-1
CONTINUUM=7.39x10^-24cm^2
(49750 cm^-1)
49750
300 K
49800
49850
49900
49950
50000
WAVENUMBER

FIG. A4.

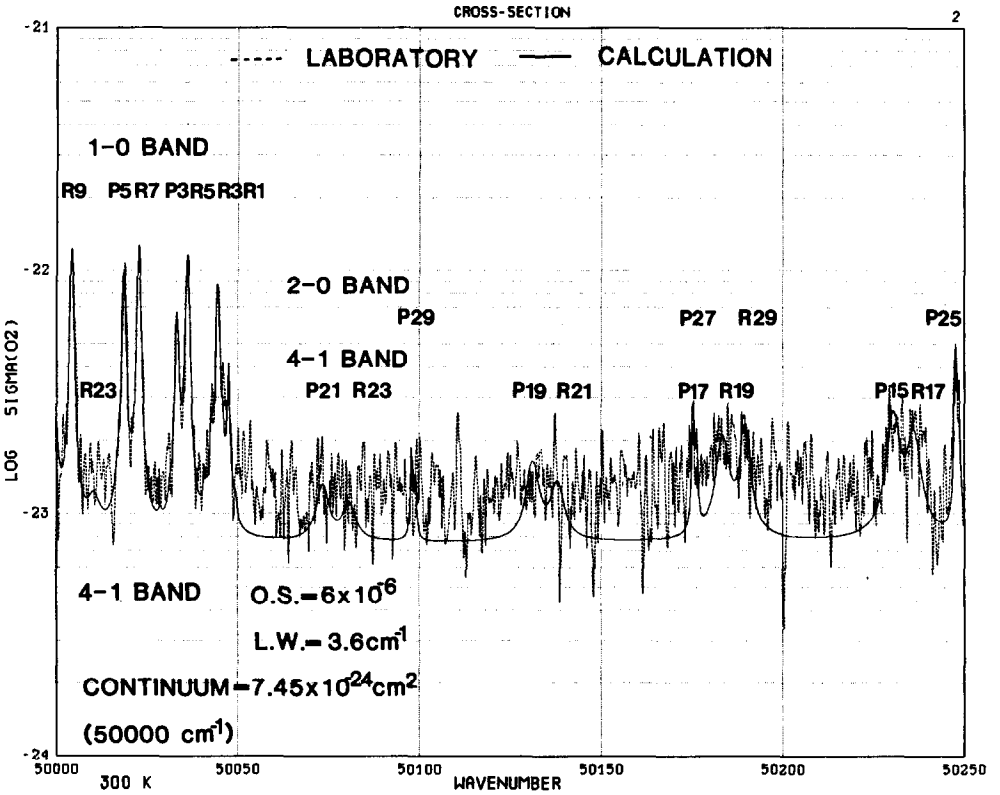
CROSS-SECTION
2
----- LABORATORY —— CALCULATION
1-0 BAND
R9 P5 R7 P3 R5 R3 R1
2-0 BAND
P29
P27 R29
P25
4-1 BAND
R23
P21 R23
P19 R21
P17 R19
P15 R17
4-1 BAND
O.S.=6x10^-6
L.W.=3.6cm^-1
CONTINUUM=7.45x10^24cm^2
(50000 cm^-1)
LOG SIGMA(O2)
-21
-22
-23
-24
50000
50050
50100
50150
50200
50250
300 K
WAVENUMBER

FIG. A5.

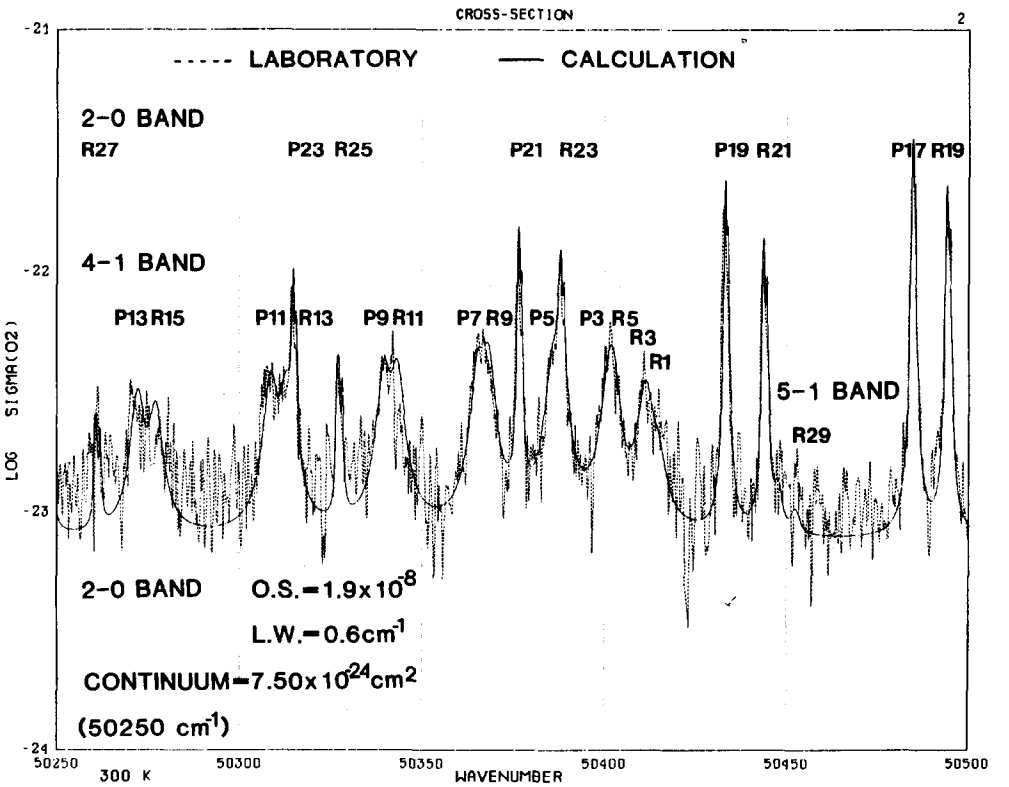
CROSS-SECTION
2
----- LABORATORY —— CALCULATION
2-0 BAND
R27
P23 R25
P21 R23
P19 R21
P17 R19
4-1 BAND
P13 R15
P11 R13
P9 R11
P7 R9
P5
P3 R5
R3
R1
5-1 BAND
R29
2-0 BAND
O.S.=1.9x10^-8
L.W.=0.6cm^-1
CONTINUUM=7.50x10^24cm^2
(50250 cm^-1)
LOG SIGMA(O2)
-21
-22
-23
-24
50250
50300
50350
50400
50450
50500
300 K
WAVENUMBER

FIG. A6.

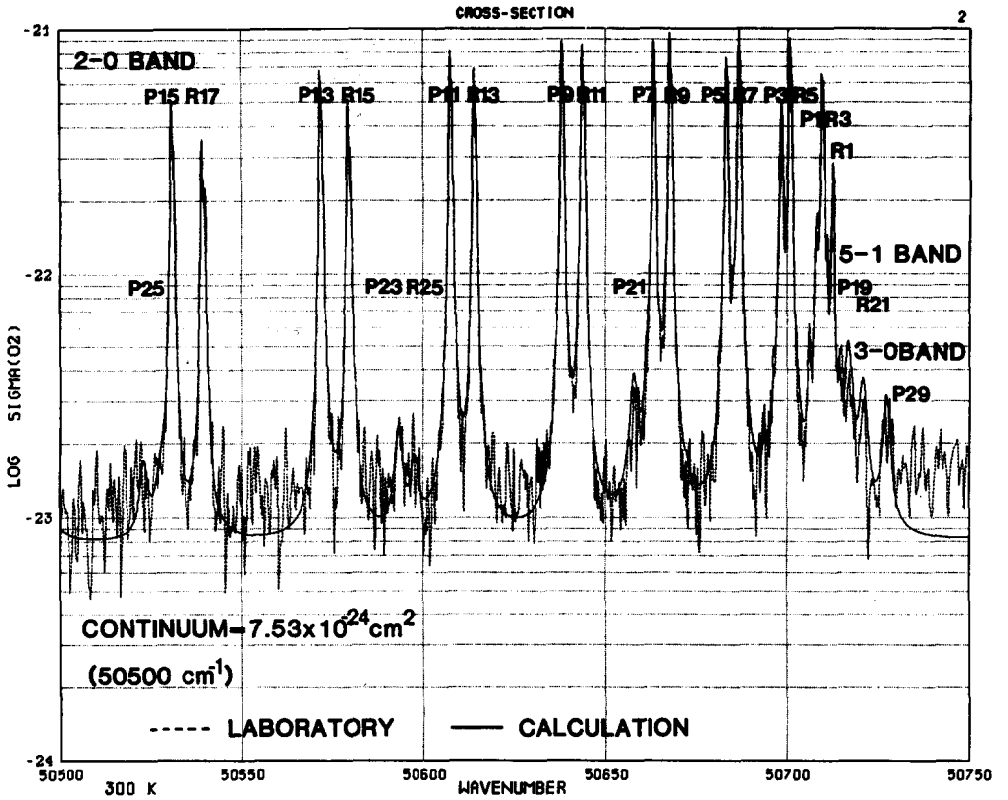
CROSS-SECTION
2
2-0 BAND
P15 R17
P13 R15
P11 R13
P9 R11
P7 R9 P5 R7 P3 R5
P1 R3
R1
5-1 BAND
P25
P23 R25
P21
P19
R21
3-0BAND
P29
CONTINUUM=7.53x10^-24 cm^2
(50500 cm^-1)
----- LABORATORY
—— CALCULATION
LOG SIGMA(O2)
-21
-22
-23
-24
50500
50550
50600
50650
50700
50750
300 K
WAVENUMBER

FIG. A7.

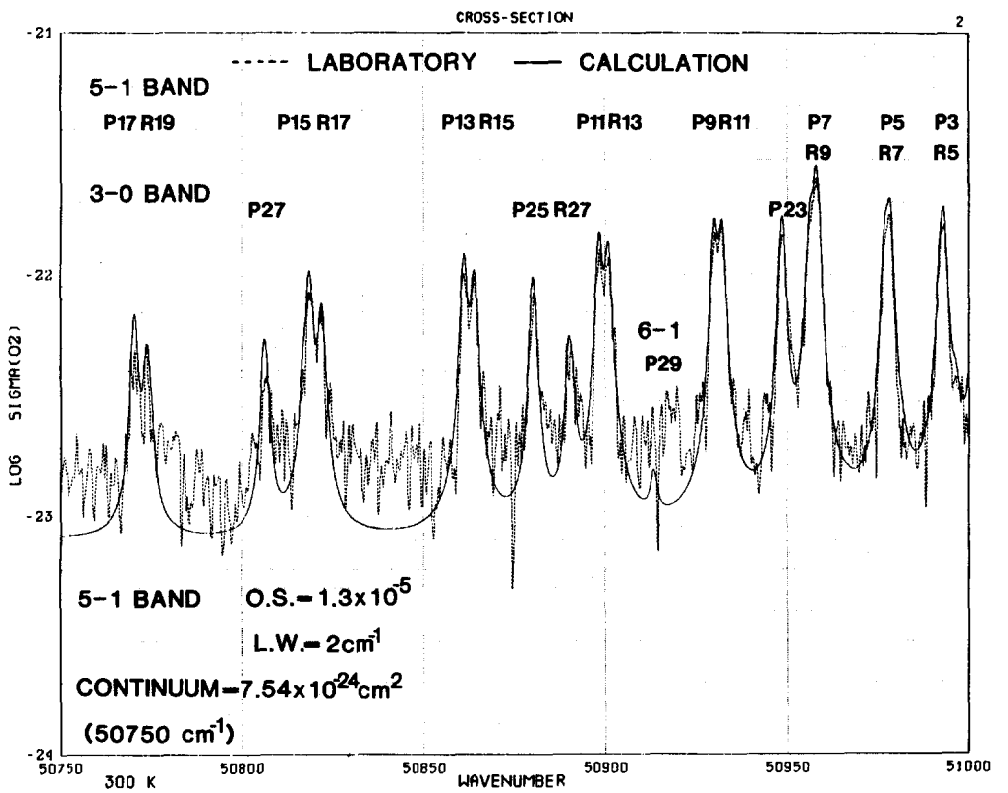
CROSS-SECTION
2
----- LABORATORY
—— CALCULATION
5-1 BAND
P17 R19
P15 R17
P13 R15
P11 R13
P9 R11
P7
R9
P5
R7
P3
R5
3-0 BAND
P27
P25 R27
P23
6-1
P29
5-1 BAND
O.S.=1.3x10^-5
L.W.=2cm^-1
CONTINUUM=7.54x10^-24 cm^2
(50750 cm^-1)
LOG SIGMA(O2)
-21
-22
-23
-24
50750
50800
50850
50900
50950
51000
300 K
WAVENUMBER

FIG. A8.

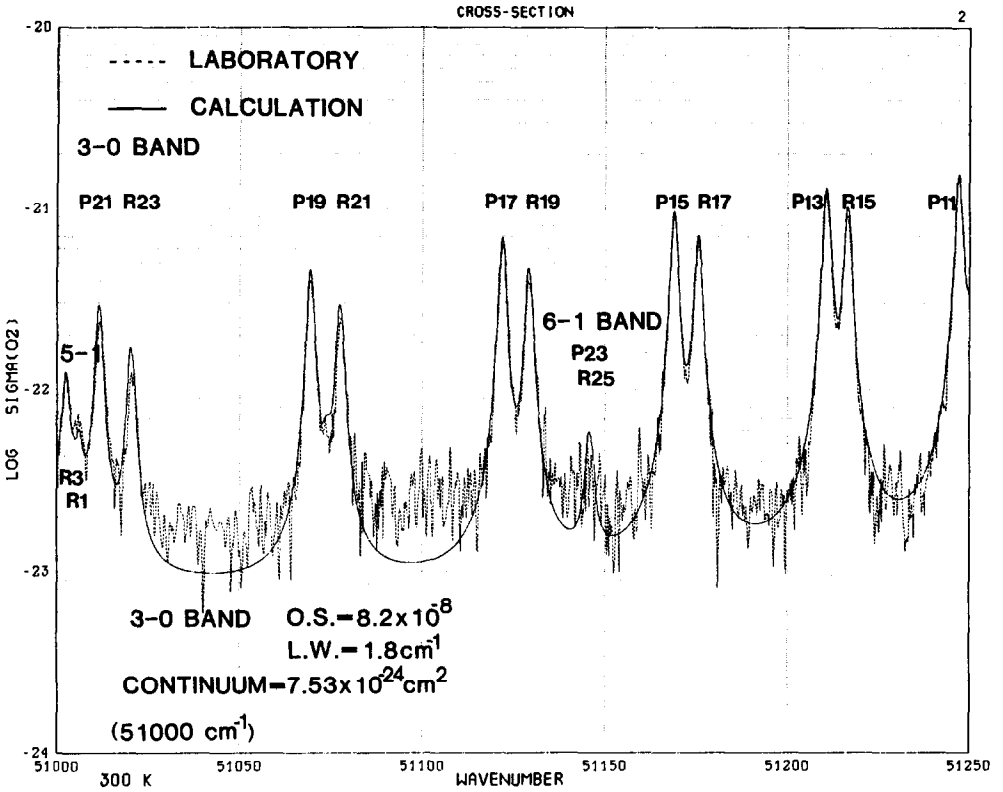

FIG. A9.

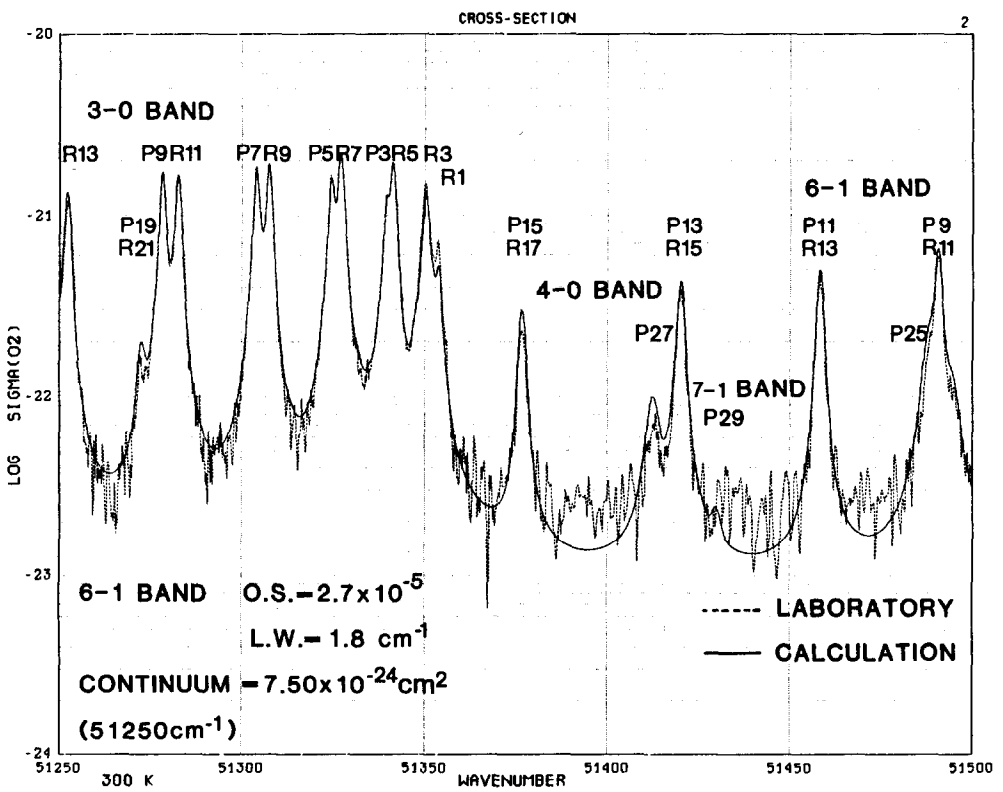

FIG. A10.

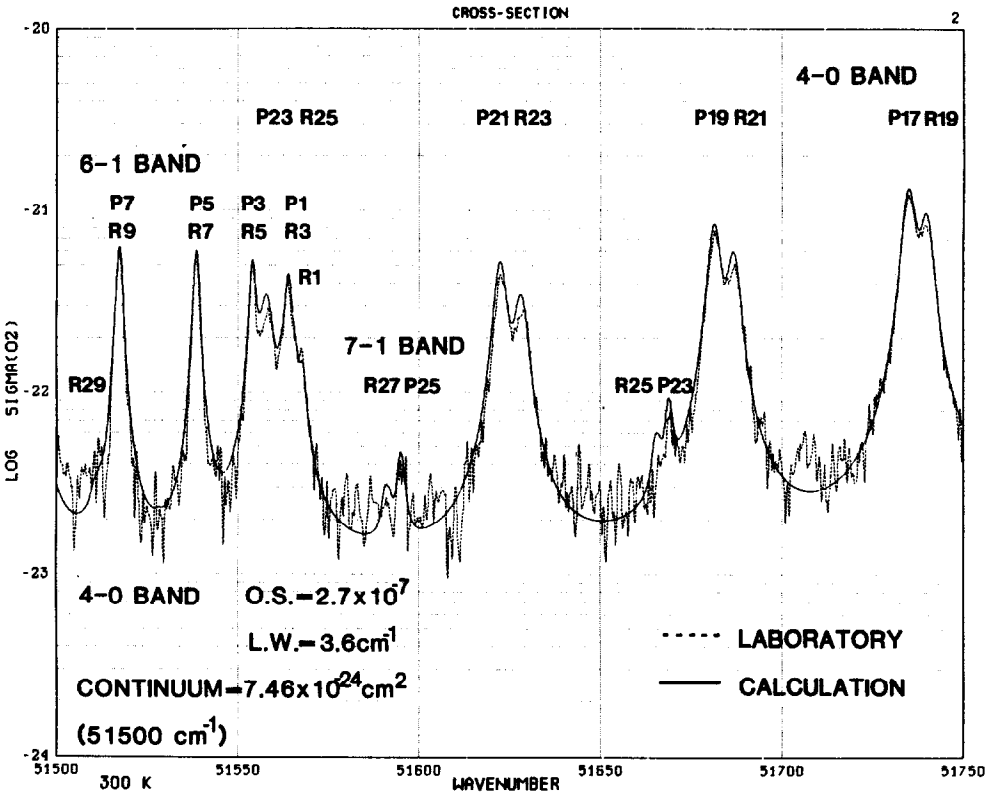

FIG. A11.

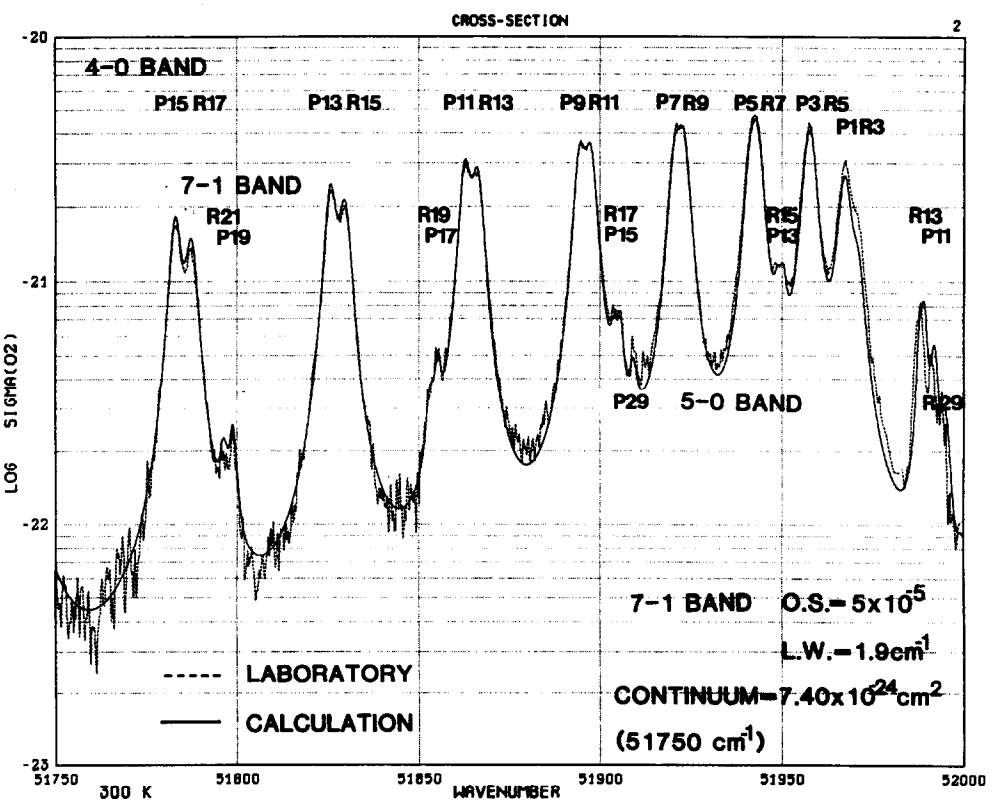

FIG. A12.

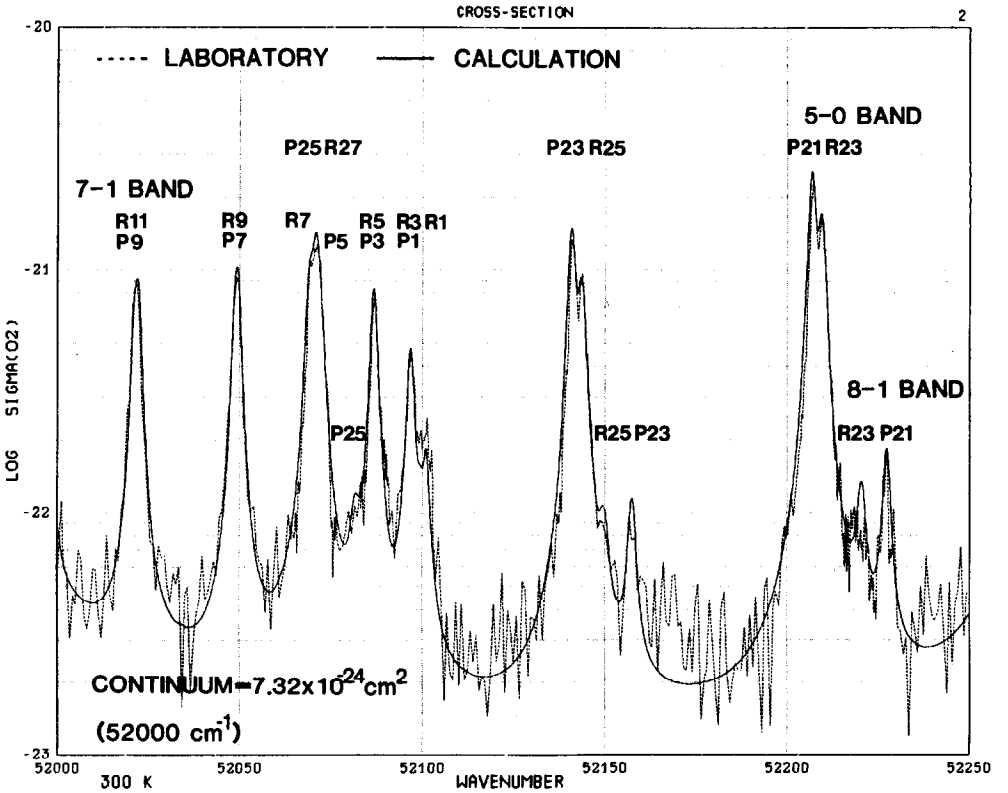

FIG. A13.

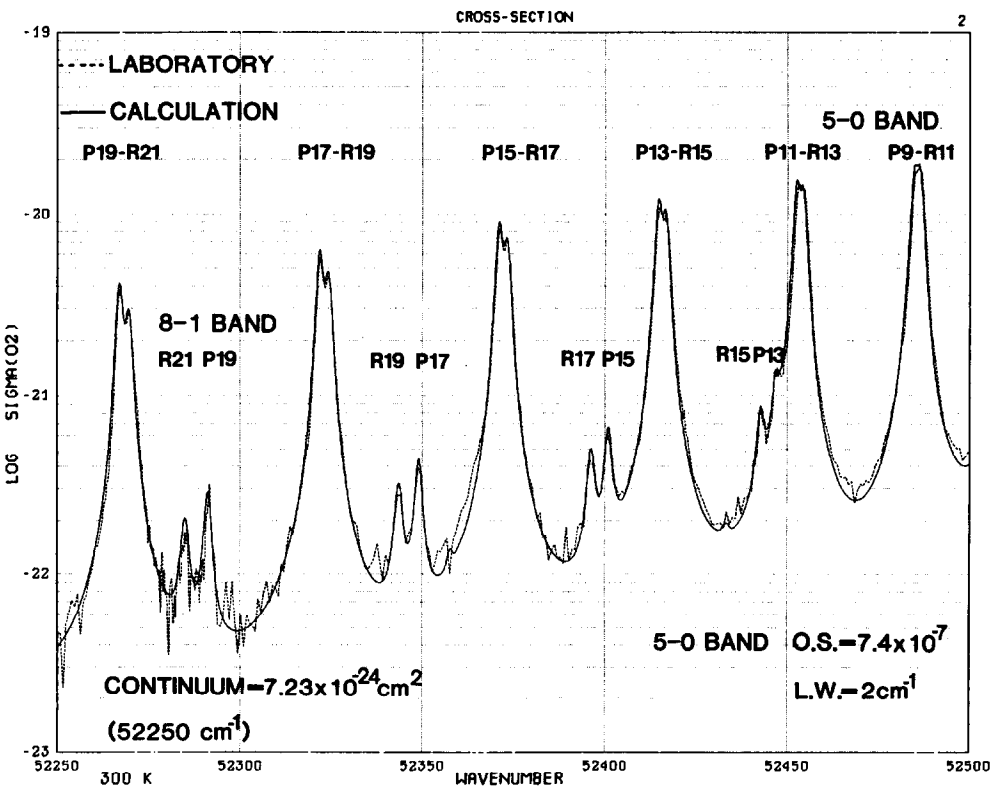

FIG. A14.

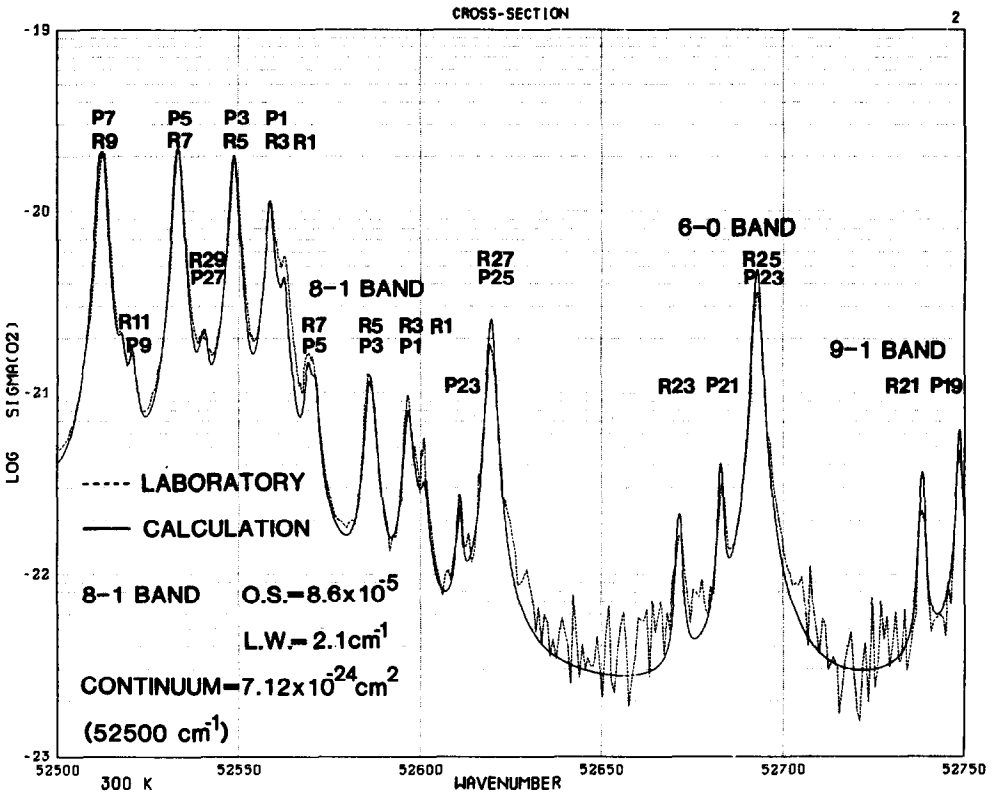

FIG. A15.

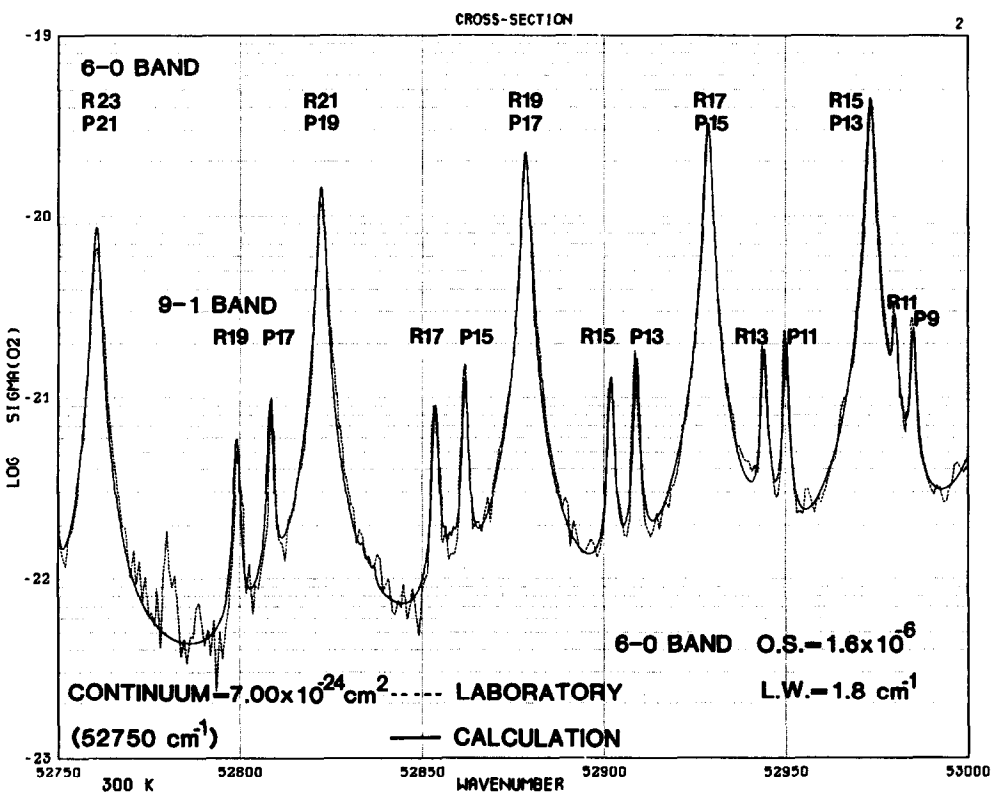

FIG. A16.

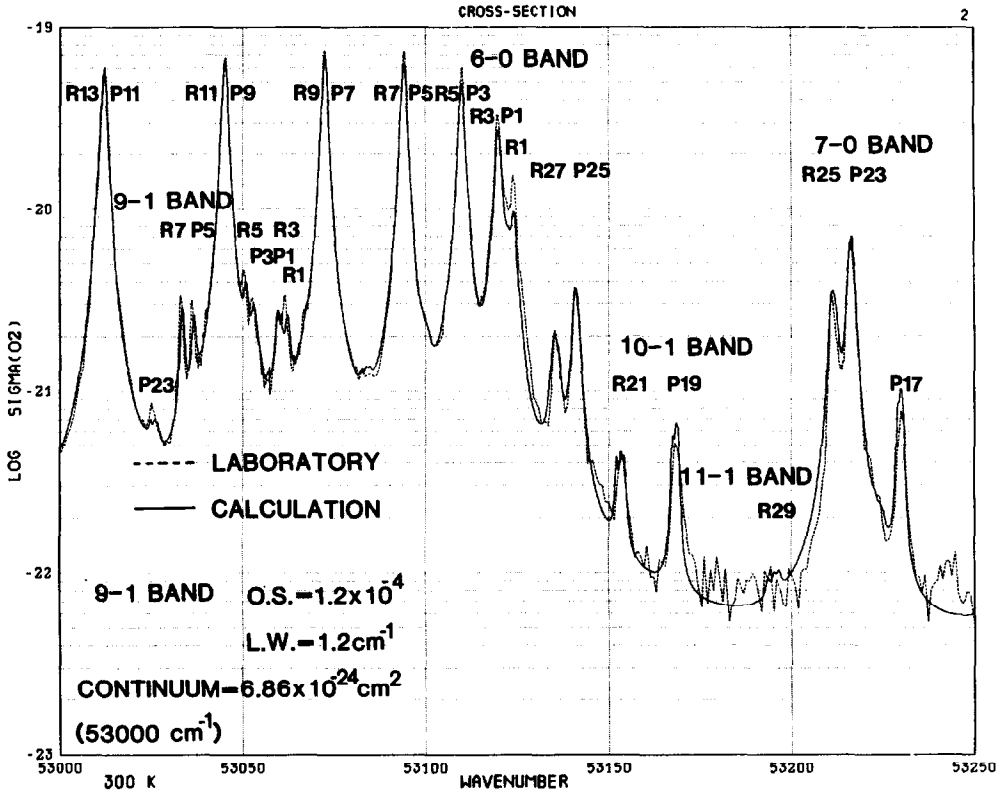

FIG. A17.

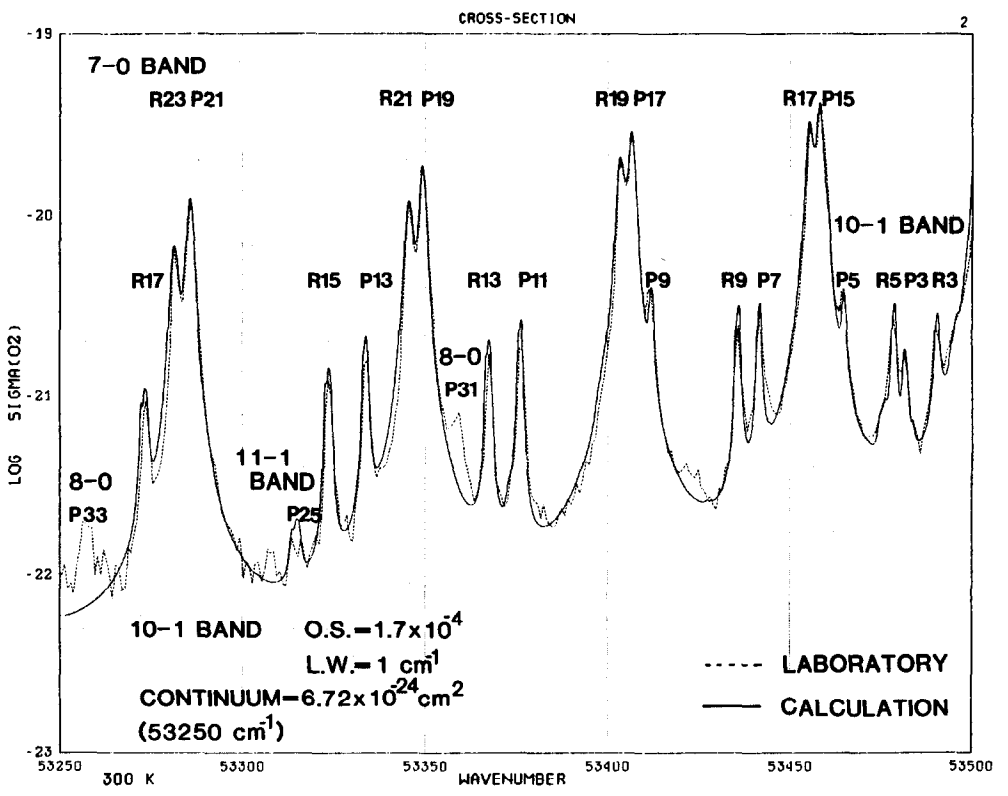

FIG. A18.

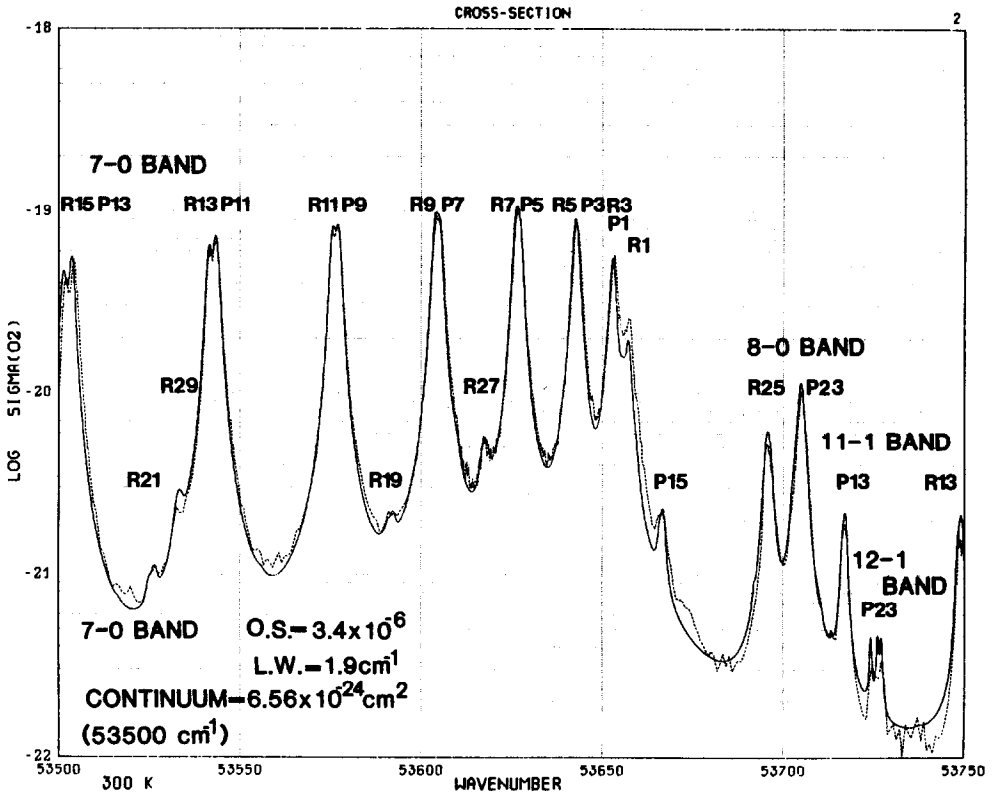

FIG. A19.

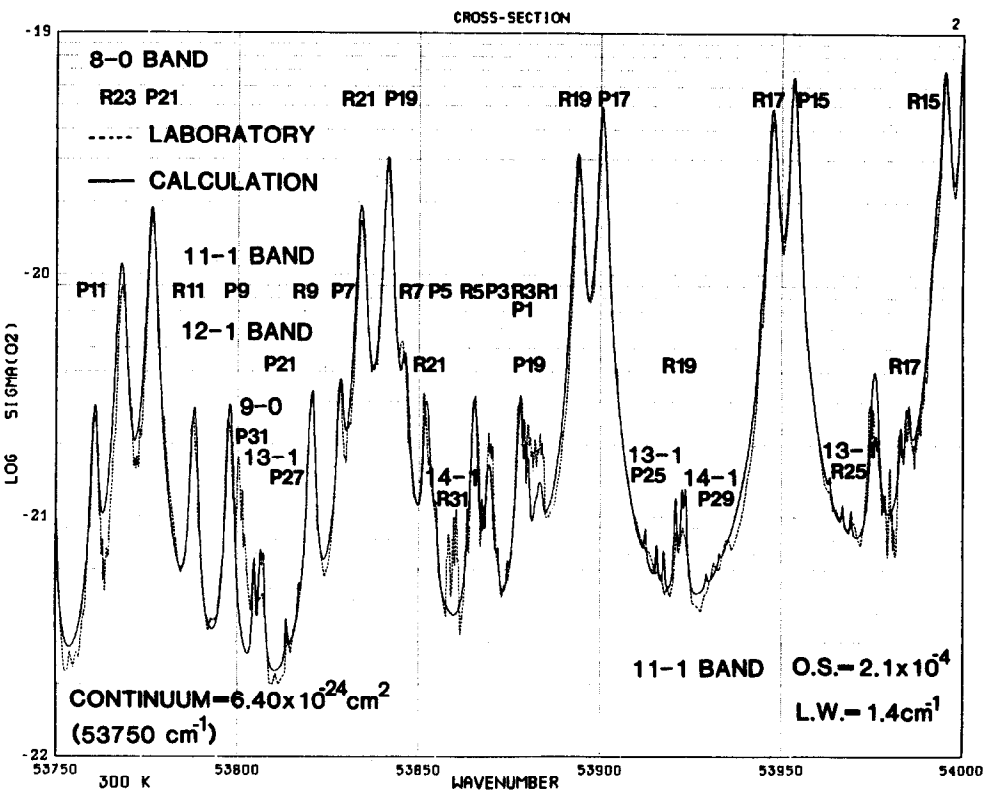

FIG. A20.

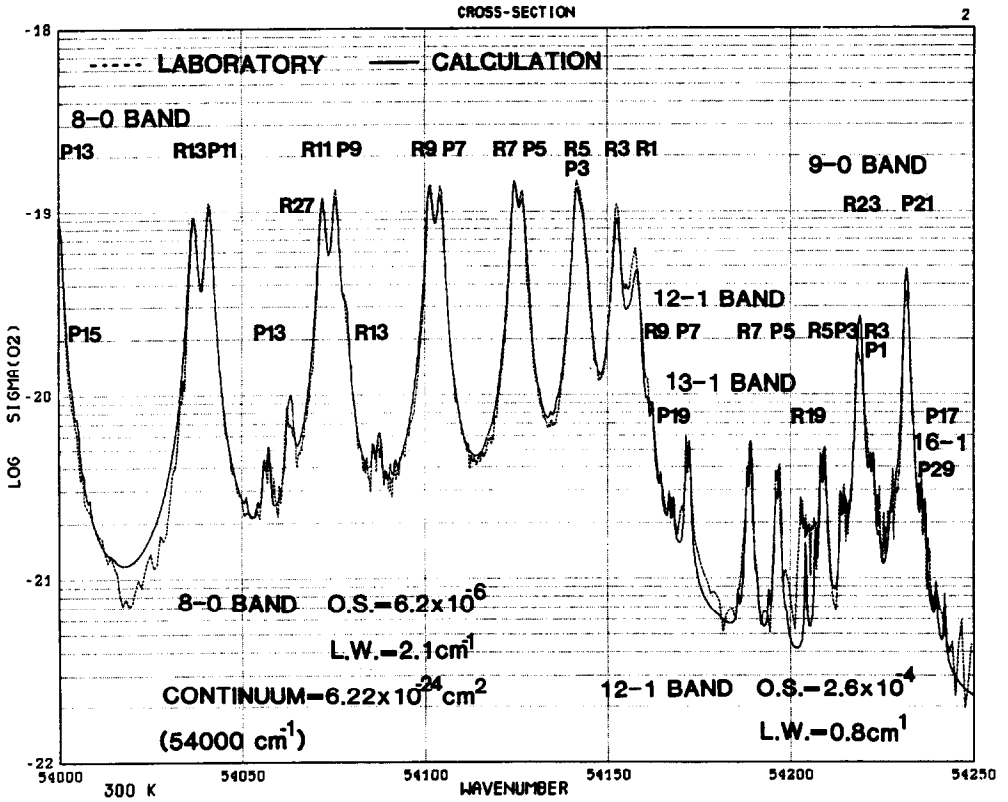

FIG. A21.

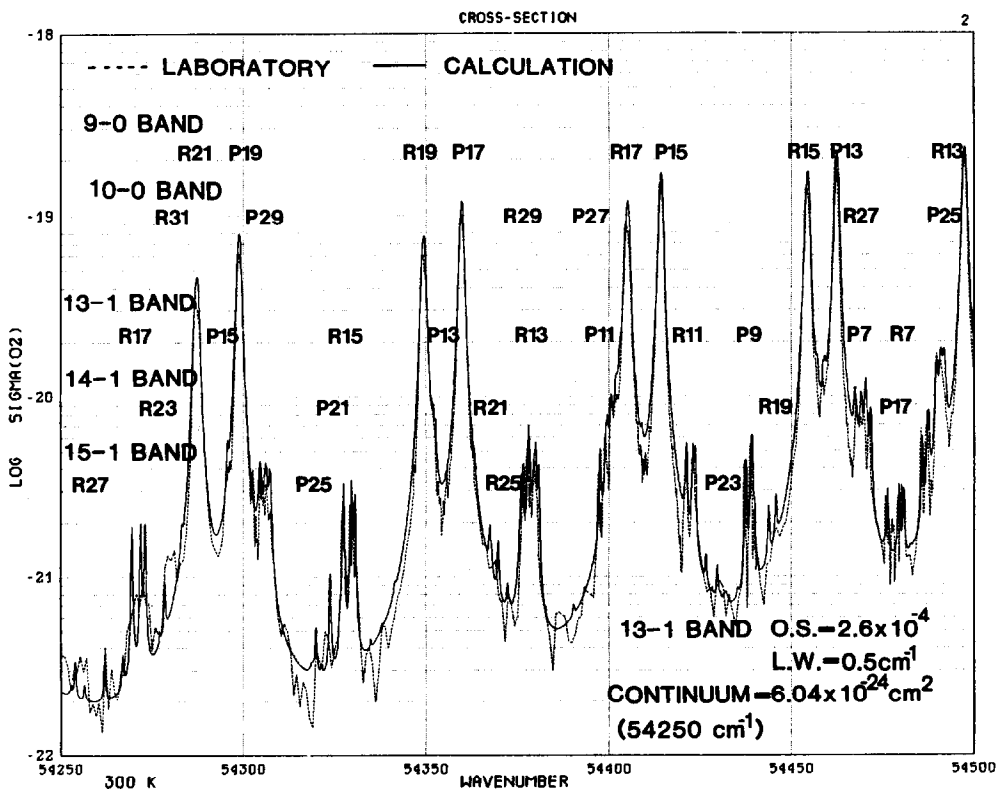

FIG. A22.

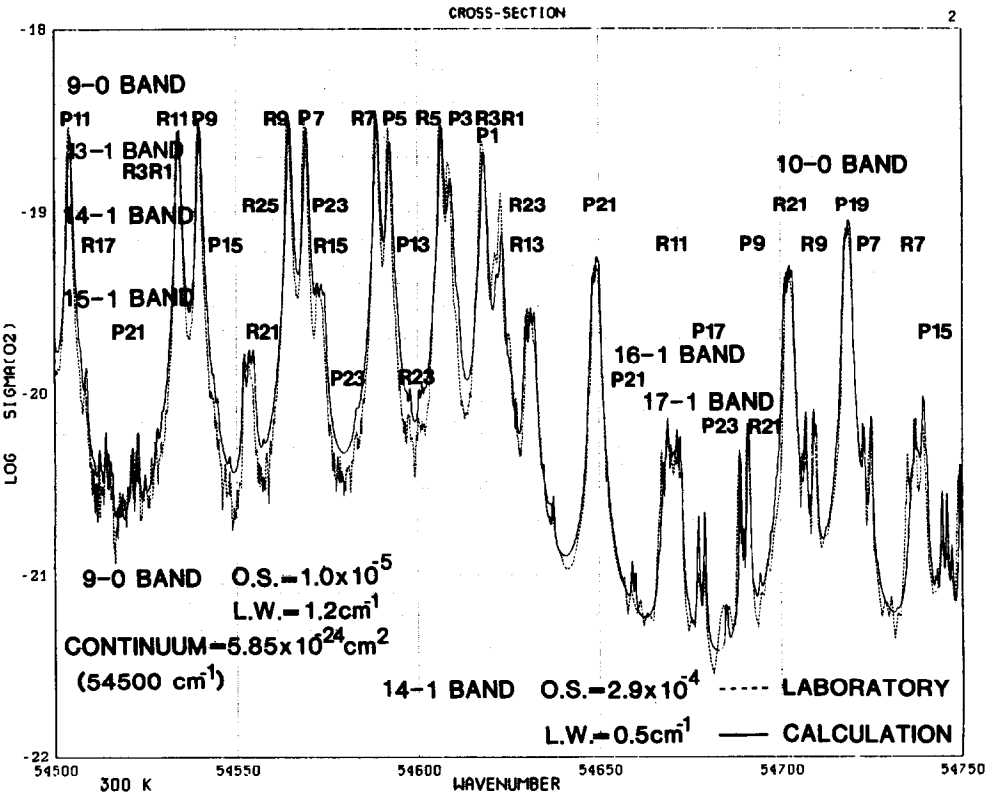

FIG. A23.

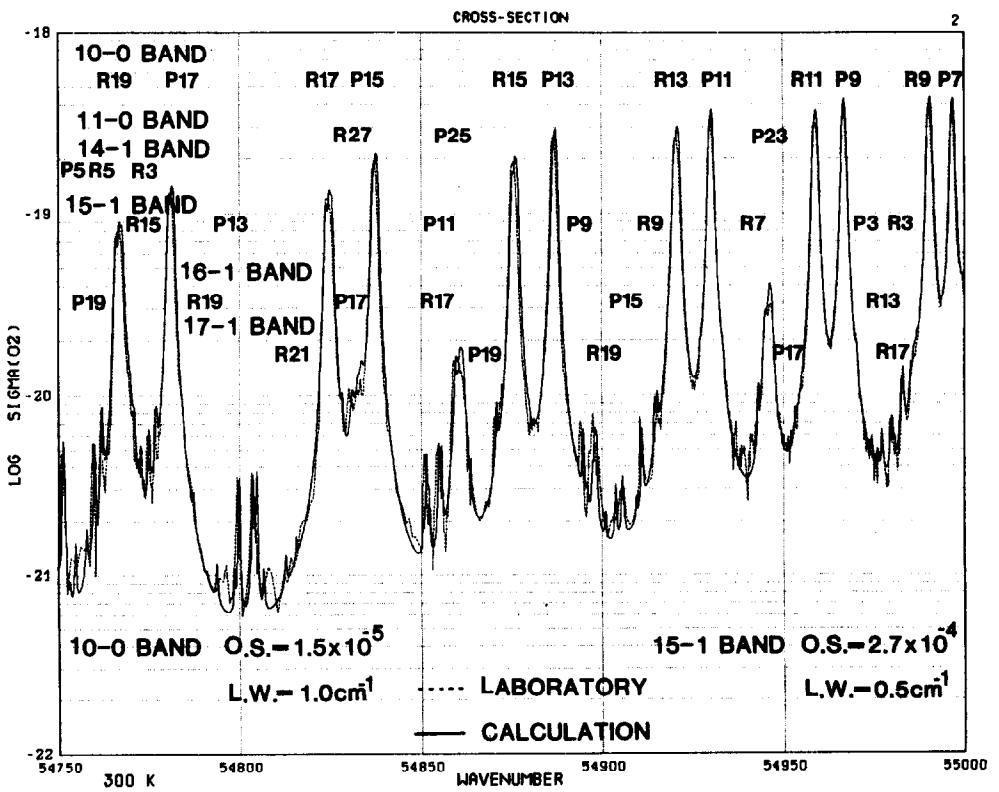

FIG. A24.

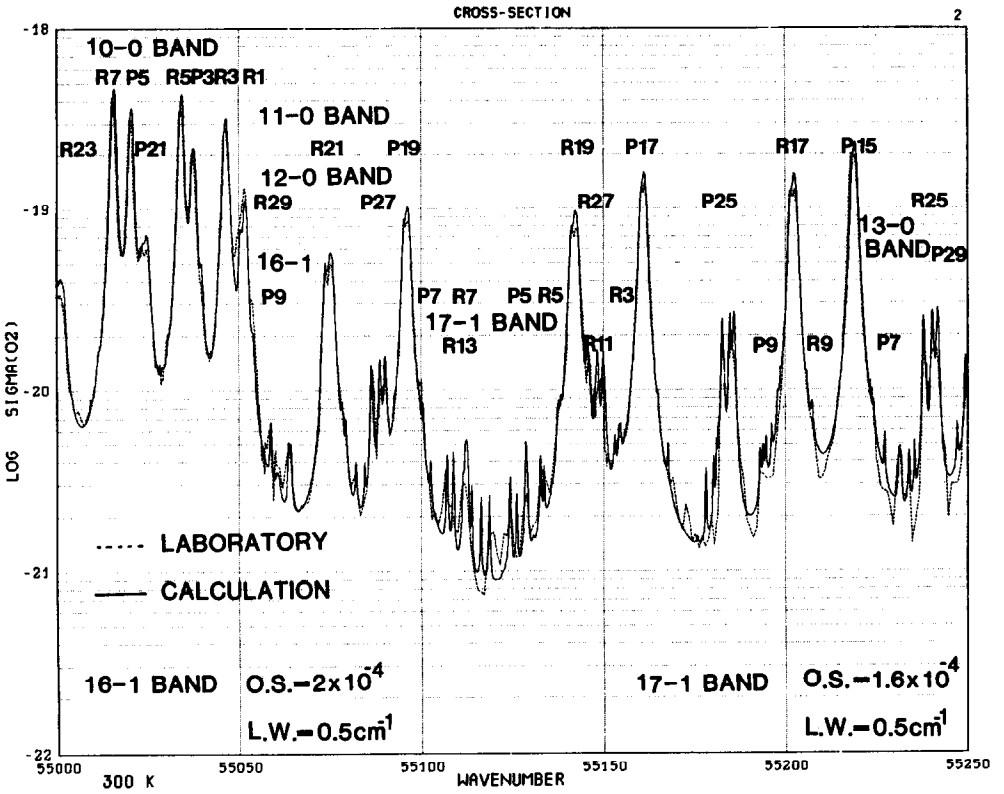

FIG. A25.

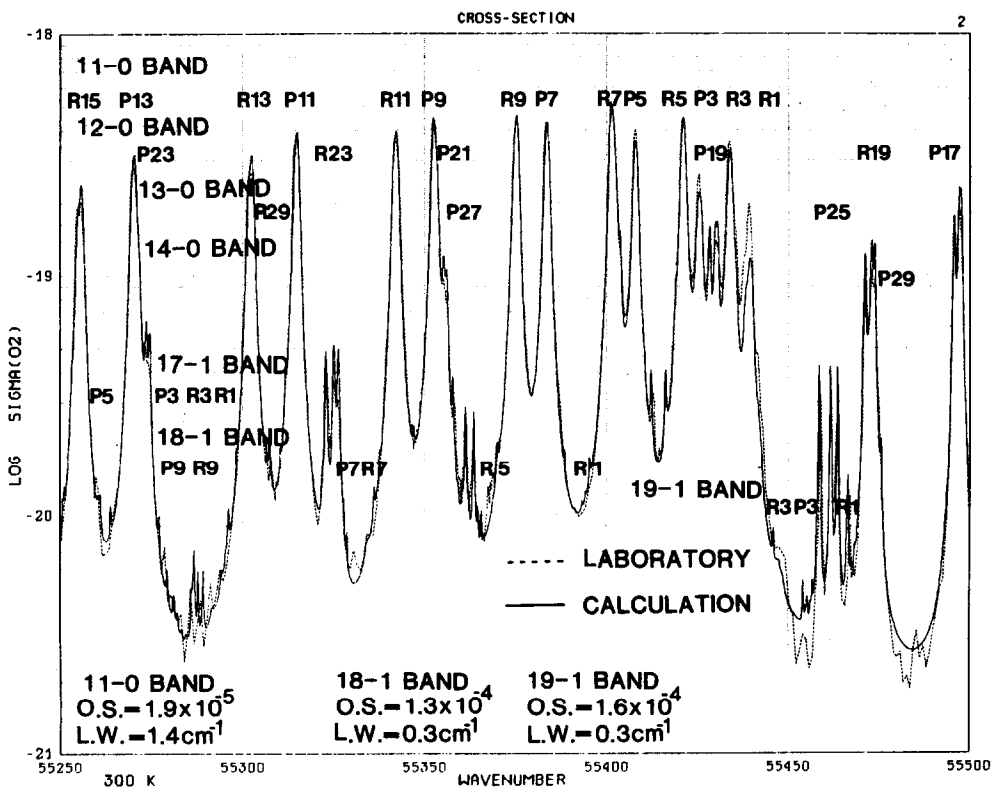

FIG. A26.

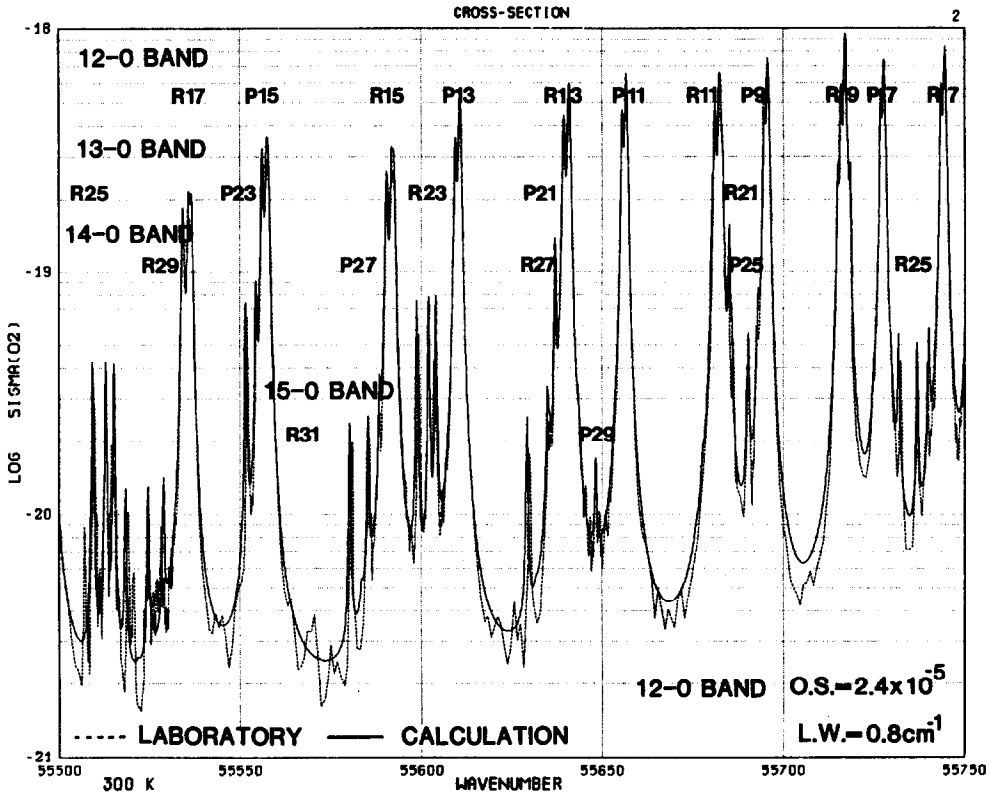

FIG. A27.

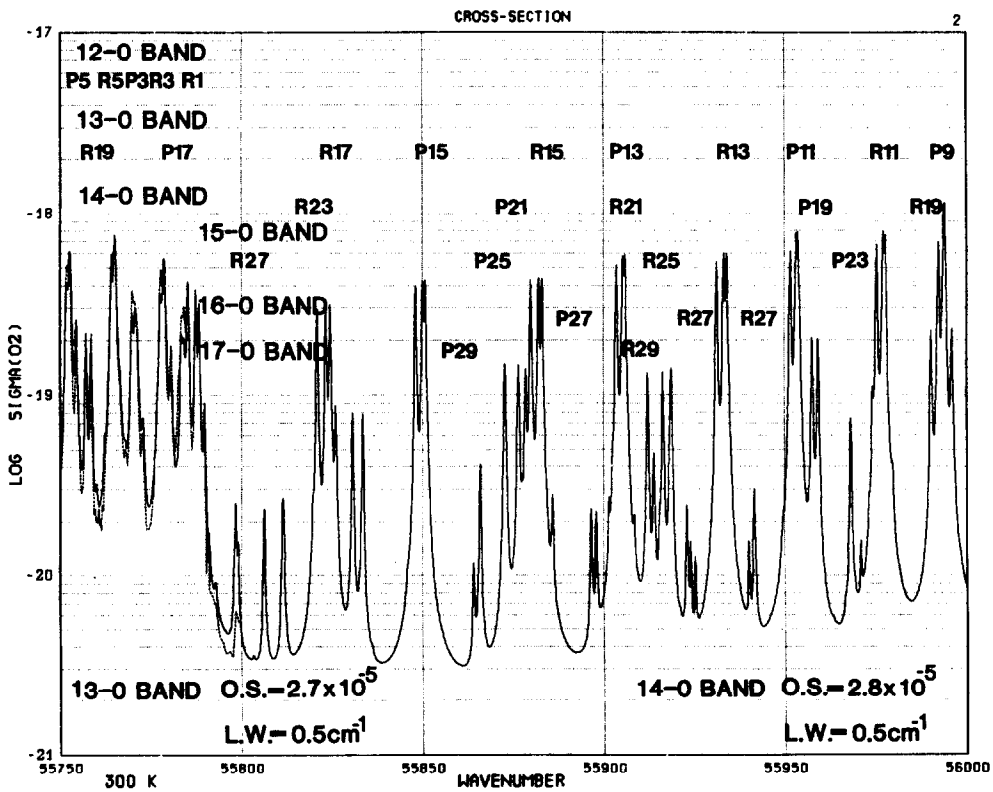

FIG. A28.

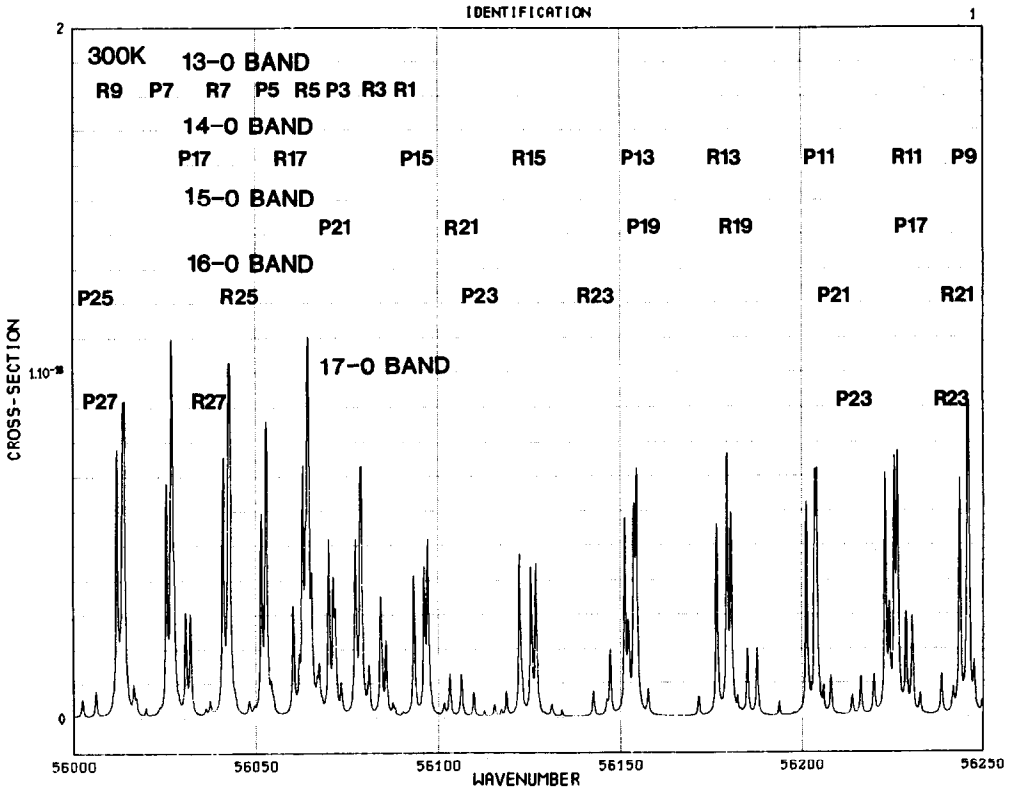
IDENTIFICATION
300K
13-0 BAND
R9 P7 R7 P5 R5 P3 R3 R1
14-0 BAND
P17 R17 P15 R15 P13 R13 P11 R11 P9
15-0 BAND
P21 R21 P19 R19 P17
16-0 BAND
P25 R25 P23 R23 P21 R21
17-0 BAND
P27 R27 P23 R23
CROSS-SECTION
56000
56050
56100
56150
56200
56250
WAVENUMBER

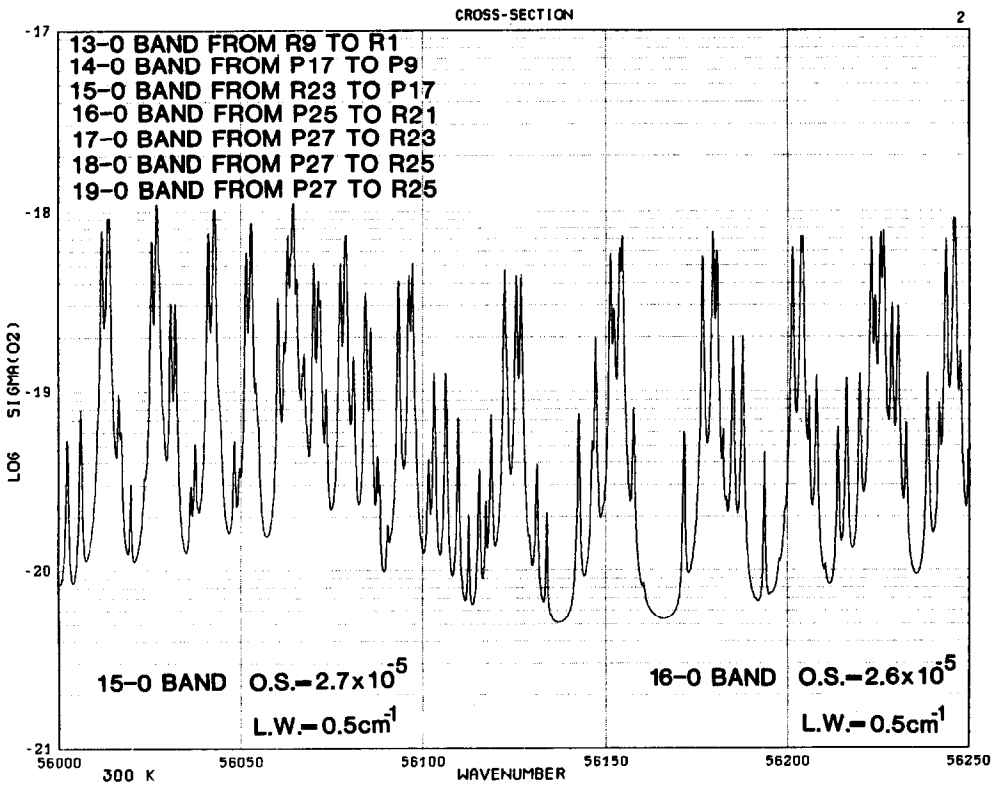
CROSS-SECTION
13-0 BAND FROM R9 TO R1
14-0 BAND FROM P17 TO P9
15-0 BAND FROM R23 TO P17
16-0 BAND FROM P25 TO R21
17-0 BAND FROM P27 TO R23
18-0 BAND FROM P27 TO R25
19-0 BAND FROM P27 TO R25
LOG SIGMA(O2)
15-0 BAND O.S.=2.7x10^-5
L.W.=0.5cm^-1
16-0 BAND O.S.=2.6x10^-5
L.W.=0.5cm^-1
300 K
WAVENUMBER

FIG. A29.

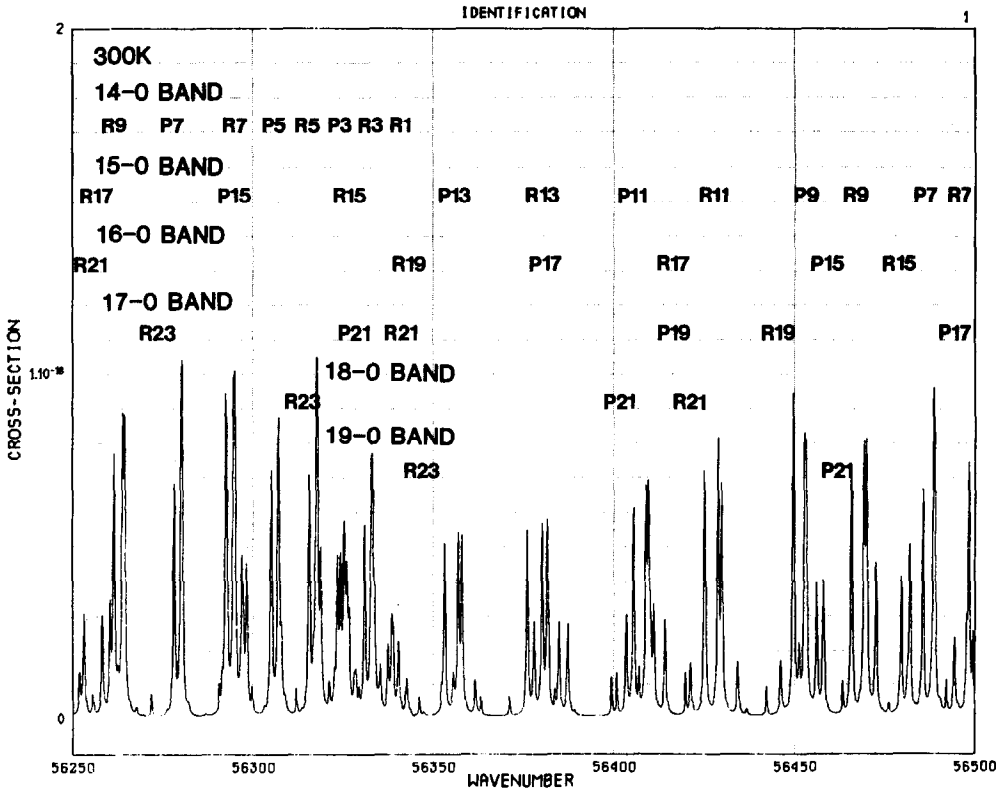
IDENTIFICATION
300K
14-0 BAND
R9 P7 R7 P5 R5 P3 R3 R1
15-0 BAND
R17 P15 R15 P13 R13 P11 R11 P9 R9 P7 R7
16-0 BAND
R21 R19 P17 R17 P15 R15
17-0 BAND
R23 P21 R21 P19 R19 P17
18-0 BAND
R23 P21 R21
19-0 BAND
R23 P21
CROSS-SECTION
WAVENUMBER
56250
56300
56350
56400
56450
56500

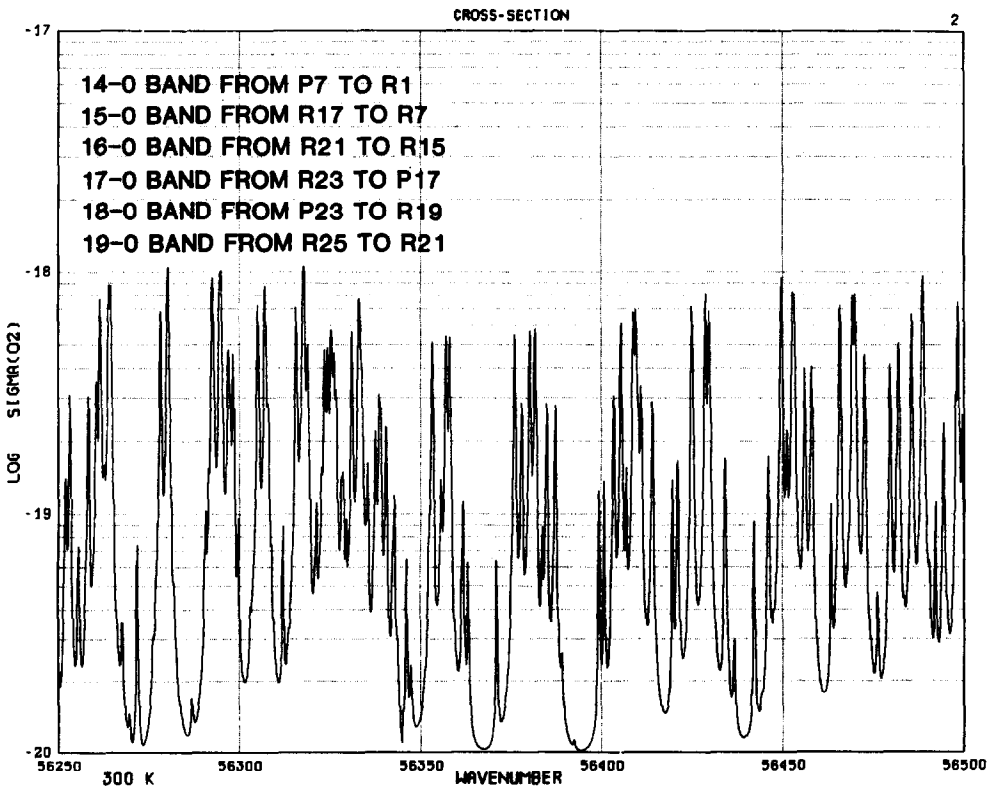
CROSS-SECTION
14-0 BAND FROM P7 TO R1
15-0 BAND FROM R17 TO R7
16-0 BAND FROM R21 TO R15
17-0 BAND FROM R23 TO P17
18-0 BAND FROM P23 TO R19
19-0 BAND FROM R25 TO R21
LOG SIGMA(O2)
-17
-18
-19
-20
300 K
WAVENUMBER
56250
56300
56350
56400
56450
56500

FIG. A30.

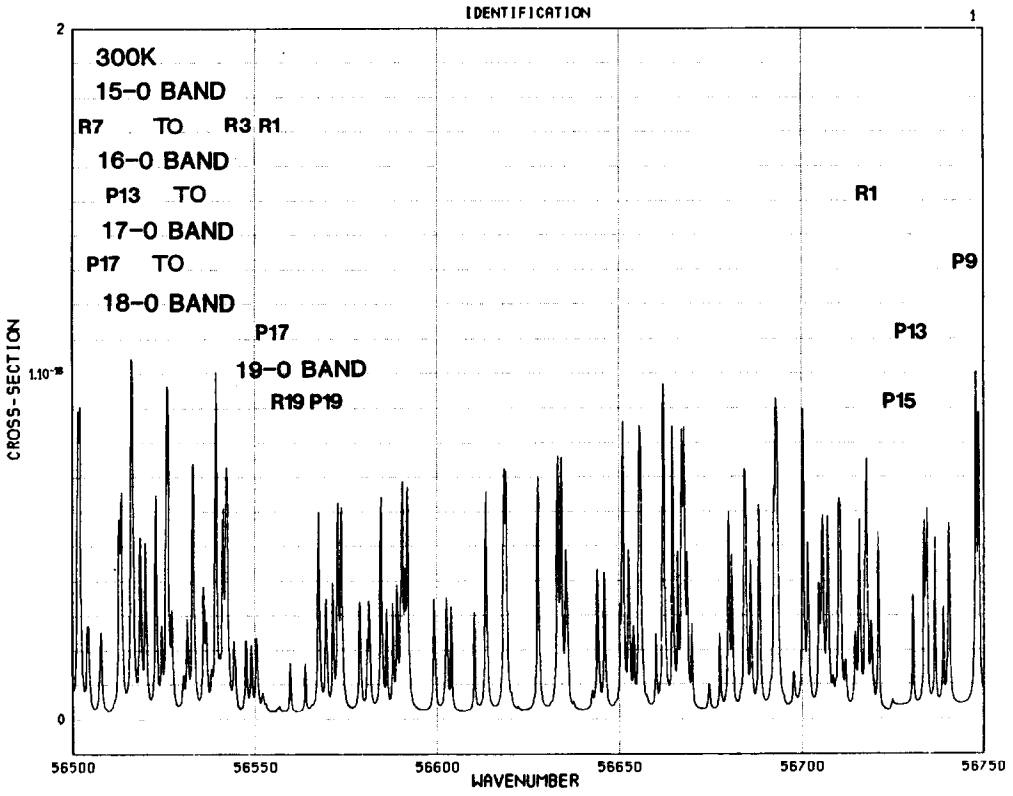
IDENTIFICATION
2
1
300K
15-0 BAND
R7 TO R3 R1
16-0 BAND
P13 TO
17-0 BAND
P17 TO
18-0 BAND
P17
19-0 BAND
R19 P19
R1
P9
P13
P15
CROSS-SECTION
1.10⁻¹⁸
0
56500
56550
56600
56650
56700
56750
WAVENUMBER

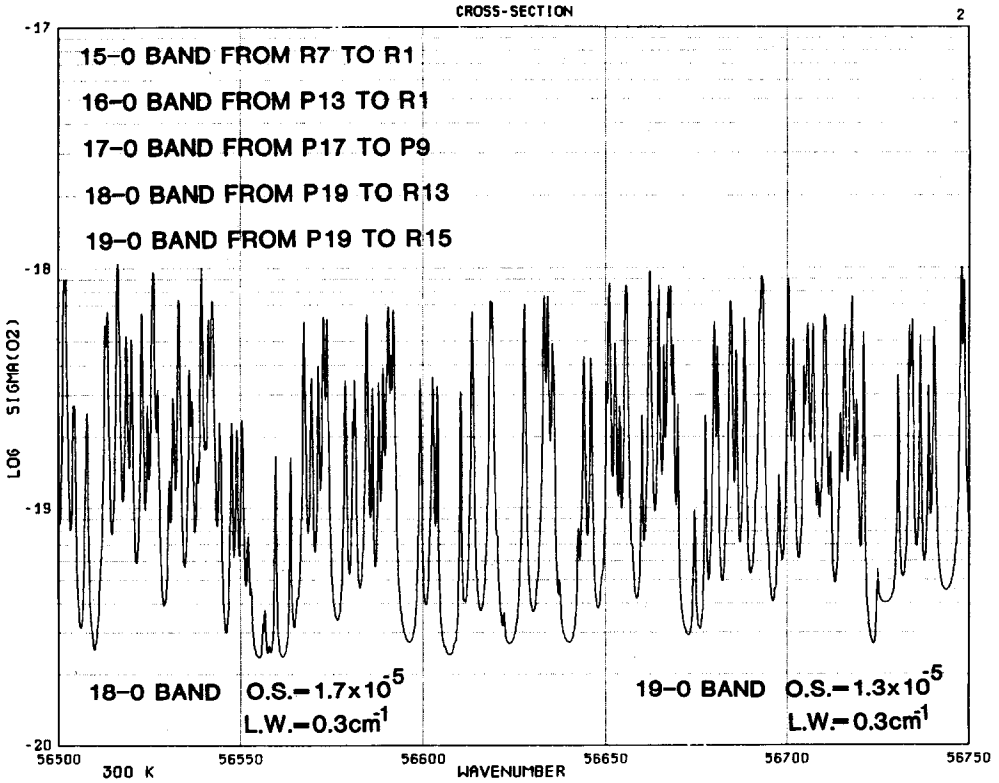
CROSS-SECTION
2
-17
15-0 BAND FROM R7 TO R1
16-0 BAND FROM P13 TO R1
17-0 BAND FROM P17 TO P9
18-0 BAND FROM P19 TO R13
19-0 BAND FROM P19 TO R15
-18
-19
-20
LOG SIGMA(O2)
18-0 BAND O.S.=1.7x10⁻⁵
L.W.=0.3cm⁻¹
19-0 BAND O.S.=1.3x10⁻⁵
L.W.=0.3cm⁻¹
300 K
56500
56550
56600
56650
56700
56750
WAVENUMBER

FIG. A31.

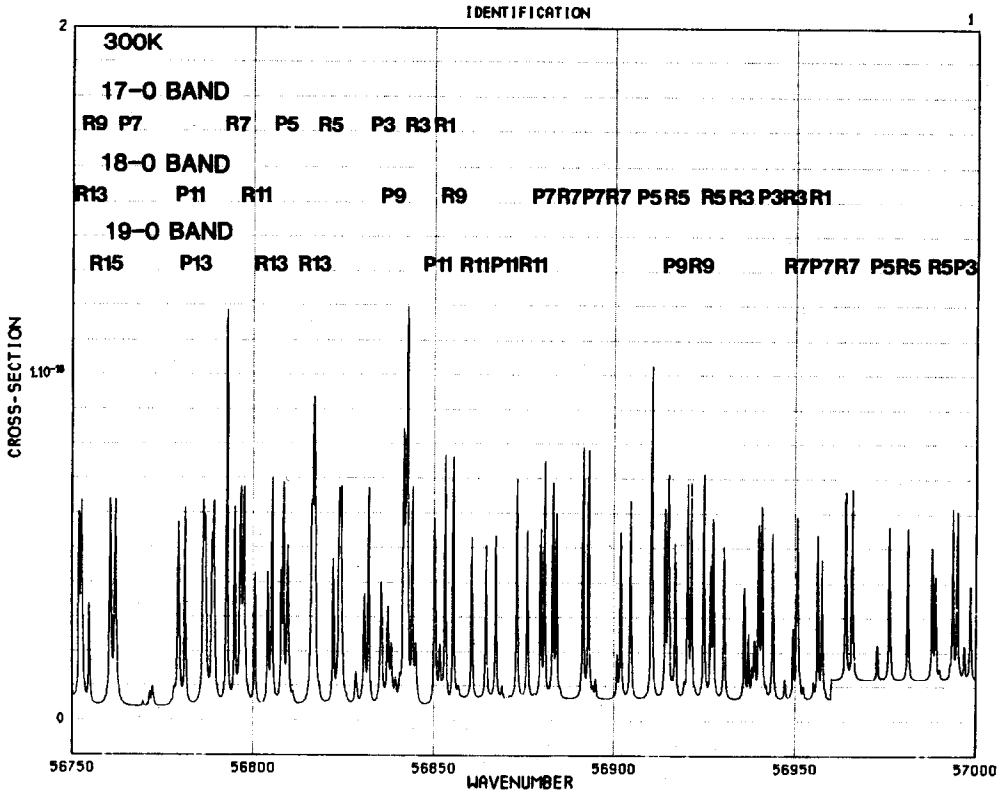
IDENTIFICATION
300K
17-0 BAND
R9 P7 R7 P5 R5 P3 R3 R1
18-0 BAND
R13 P11 R11 P9 R9 P7R7P7R7 P5R5 R5R3 P3R3R1
19-0 BAND
R15 P13 R13 R13 P11 R11P11R11 P9R9 R7P7R7 P5R5 R5P3
CROSS-SECTION
0
56750
56800
56850
56900
56950
57000
WAVENUMBER

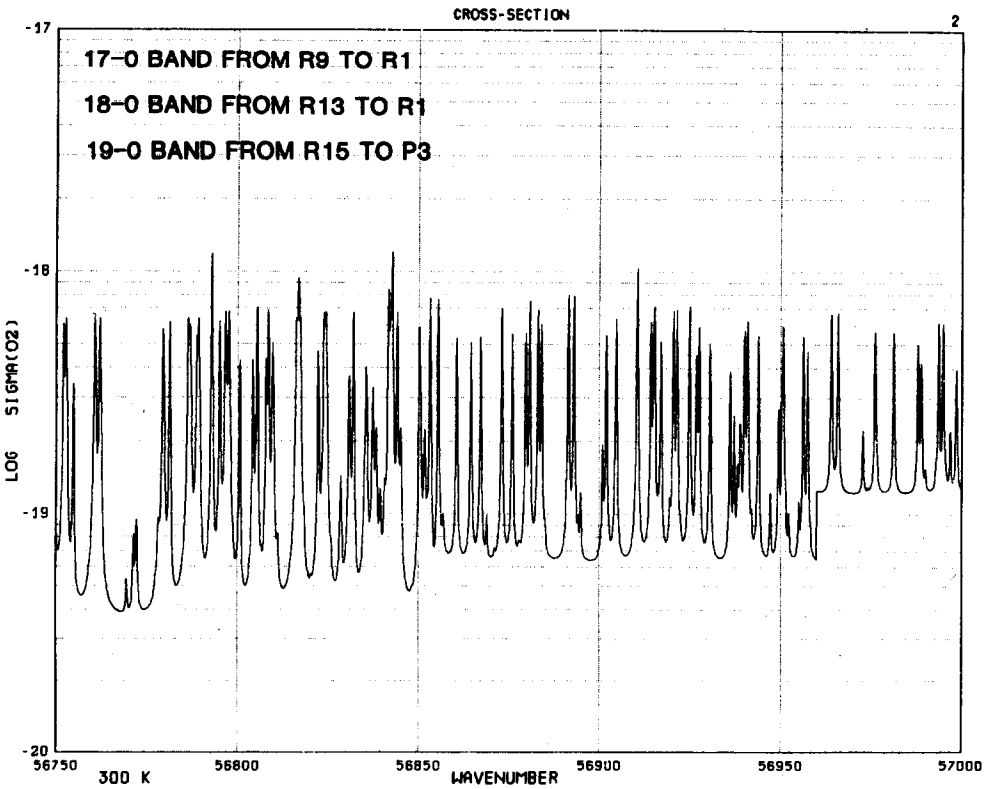
CROSS-SECTION
17-0 BAND FROM R9 TO R1
18-0 BAND FROM R13 TO R1
19-0 BAND FROM R15 TO P3
LOG SIGMA(O2)
-17
-18
-19
-20
300 K
56750
56800
56850
56900
56950
57000
WAVENUMBER

FIG. A32.

Rotational constants of the upper electronic state of the Schumann–Runge system have also been published recently by Cheung *et al.* (1986). These constants open the possibility of calculating the wavenumbers of the rotational lines. The same spectroscopic constants have also been determined by Lewis (1986a) from the wavenumber measurements of Yoshino *et al.* (1984).

The band oscillator strengths of the $(v', 0)$ and $(v', 1)$ bands adopted here are based on the various results of Yoshino *et al.* (1983), of Cheung *et al.* (1984), of Yoshino *et al.* (1987), of Lewis (1986a), and also of Allison *et al.* (1971).

The predissociation linewidths have been determined after detailed comparison between calculated absorption cross-sections and the experimental results published by Yoshino *et al.* (1983) in the spectral region corresponding to the $v' = 1$–12 bands. However, the absorption cross-sections throughout this region may also depend on the underlying continuum that corresponds near 50,000 cm^{-1} to the O_2 Herzberg continuum (see Nicolet and Kennes, 1986, 1988). At wavenumbers greater than 55,000 cm^{-1}, the O_2 Schumann–Runge continuum (see Lewis, *et al.* (1985a,b) plays a role that is dependent on temperature.

The rotational structure of the bands

The Schumann–Runge bands of O_2 arise from the transition $B\ ^3\Sigma_u^- - X\ ^3\Sigma_g^-$ in the 49,000–57,000 cm^{-1} spectral region containing the rotational lines from bands with $v' = 0$–19 and $v'' = 0$ and 1 in absorption when the temperature is not more than 300 K. From 2–0 to 19–0, the intervals decrease from 665 to 75 cm^{-1}; these values correspond to a variation from 2.62 to 0.23 nm. The absorption occurs mostly in the six principal branches, *P* and *R*. The final results of the calculations illustrate that the distribution of the intensity varies greatly in each interval. However, at low temperature, the structure is different, because the rotational lines of the bands with $v'' = 1$ do not play any role at low temperature; the rotational structure represents at low temperature only the bands from $v'' = 0$. The maximum averaged cross-sections for 500 cm^{-1} intervals vary from about 8×10^{-24} cm^2 between 49,000–49,500 cm^{-1} (practically the underlying continuum) to almost 2×10^{-19} cm^2 between 56,500–57,000 cm^{-1}, the spectral range of the 15–0–19–0 bands. The variation of 10^4 in the absorption cross-sections (10^{-23}–10^{-19} cm^2) requires that atmospheric absorption be taken into account from the mesopause to the lower stratosphere, for temperatures from 270 to less than 190 K.

The O_2 Herzberg continuum

The absorption cross-sections of the O_2 Herzberg continuum at wavelengths greater than 200 nm that were used before 1980 must now be replaced by experimental and observational results obtained recently (1984–1986). An analysis by Nicolet and Kennes (1986, 1988) leads to the adoption of an empirical formula for the absorption cross-section, $\sigma_{HER}(O_2)$ cm^2,

$$\sigma_{HER}(O_2) = 7.5 \times 10^{-24}(\nu/5 \times 10^4) \times \exp\{-50[\ln(\nu/5 \times 10^4)]^2\}$$

The O_2 Schumann–Runge continuum

The photoabsorption continuum underlying the Schumann–Runge bands of vibration $v' > 10$ has been deduced almost exclusively from recent analysis (Lewis *et al.*, 1985a,b).

The values from our approximate determination of the cross-sections were deduced for temperatures between 170 and 300 K, corresponding to the range of atmospheric and laboratory temperatures. This continuum is affected by the rotational and vibrational populations, and is subject to strong variation with temperature and wavelength. The following averaged values of the absorption cross-section at

	55,250 cm^{-1}	and	55,750 cm^{-1}
$T = 170$ K	3.1×10^{-23} cm^2		1.6×10^{-20} cm^2
$T = 300$ K	3.0×10^{-22} cm^2		3.8×10^{-20} cm^2

reveal a difference of at least a factor of 10^3. But this influence is limited by the high absolute values of the absorption cross-section of the rotational lines.

Absorption cross-sections

The calculated absorption cross-sections of the Schumann–Runge bands of O_2 are presented in graphical format throughout the 49,000–57,000 cm^{-1} wavenumber region corresponding to all bands with $v' = 0$–19 and $v'' = 0$ and 1 for $T = 300$ K.

Our calculated ($v' = 0$–19) absorption cross-sections and the measured ($v' = 2$–12, $v'' = 0$; $v' = 3$–19, $v'' = 1$) cross-sections of Yoshino *et al.* (1983) are shown as 250 cm^{-1} semi-logarithmic plots in separate figures; the principal identifications of rotational lines correspond to the six main branches $P(N)$ and $R(N)$.

Such figures open the possibility for detailed comparison at 300 K between the calculated and measured cross-sections. However, when the cross-section between peaks of the various lines is less than 3×10^{-23}, from 49,750 to at least 51,500 cm^{-1}, the experimental structure must be assessed as due to the noise occurring in the continuum, for cross-sections up to almost 10^{-22} cm^2. When all absorption cross-sections are greater than 10^{-22} cm^2, there is excellent agreement between the absolute measured and calculated cross-sections at 300 K. Thus, in the spectral region where the absorption cross-section is less than 5×10^{-23} cm^2, the role of the underlying continuum must be given particular attention.